INVESTIGATIONS OF MACROPOROUS AND MESOPOROUS MATERIALS

A THESIS SUBMITTED IN PARTIAL FULFILMENT OF THE REQUIREMENTS OF THE DEGREE OF MASTER OF SCIENCE AS A PART OF THE INTEGRATED Ph.D. PROGRAMME

BY

GAUTAM GUNDIAH

TO

MANIPAL ACADEMY OF HIGHER EDUCATION

THROUGH

JAWAHARLAL NEHRU CENTRE FOR ADVANCED SCIENTIFIC RESEARCH, BANGALORE

MARCH 2001

STATEMENT

Certified that the work described here has been done under my supervision at Jawaharlal Nehru Centre for Advanced Scientific Research, Jakkur, Bangalore.

Prof. C.N.R. Rao

ACKNOWLEDGEMENTS

It is indeed a great pleasure to record my deep sense of gratitude and respect to Professor C.N.R. Rao, FRS, for suggesting the problem, inspiring guidance and support throughout the course of this investigation. I have learned immensely from him in tackling research problems and being positive when the going gets tough. I owe him immensely for his efforts in shaping me up as a research student and look forward to his encouragement in the years to come.

It has been a pleasure working with Dr. A. Govindaraj in Carbon Lab. His enthusiasm and hard-working nature deserve a special mention and it has been a tremendous learning experience for me.

I thank Dr. S. Natarajan for helping me during the initial stages of my research with aluminosilicates.

I would like to thank my teachers at the Chemical Sciences Division, IISc namely Profs. J. Chandrasekhar, S. Chandrasekharan, S. Ramasesha and T.N. Gururow for their guidance. Prof. V. Krishnan, Dr. W.H. Madhusudan and all the Faculty members of JNCASR are greatfully acknowledged.

My collaborators, Drs. M. Eswaramoorthy and Neeraj have been extremely helpful to me in attending to the various problems faced by me.

I thank my labmates in Frameworks Lab (Neeraj, Amitava, Vaidhya, Jayaraman and Sandip) and in Carbon Lab (Manashi and Deepak) for providing a great atmosphere of learning in the lab.

The help rendered by the technical staff of JNCASR are acknowledged. I thank Dr. Bala and other members of the Computer Lab for maintaining excellent computational facilities.

I would like to thank my Int. Ph.D seniors at JNCASR for helping me during my coursework. I was indeed fortunate to be a part of the '98 Int. Ph.D. batch and I thank my batchmates for making my stay in IISc a pleasant learning experience.

I thank my friends Vinod and Murugavel for being what they are and boosting me up whenever my morale was low. I thank Vinod and John for all the help they rendered in preparing this thesis.

My friends, namely Murugavel, Vinod, Pattu, Sujay, Sudhee, Siva, Saji, Sivashankar, Sarathy, Deepak, Arpita, Soma and many others in JNCASR have made my stay in the hostel wonderful, the memories of which I will cherish for the rest of my life.

Last but not the least, I would like to thank my family members, Amma, Praveena, Rita, Venkatesh, Sanjay and Varun for all the love and support that they have given me. They have never imposed their views on me and have allowed me to pursue the career of my choice. I would like to thank Ganga Aunty and Krishnappa Uncle for their love and affection. This acknowledgement would be incomplete without thanking Appa, who has always been a source of inspiration for me. I dedicate this thesis to his loving memory.

CONTENTS

INVESTIGATIONS OF MACROPOROUS AND MESOPOROUS MATERIALS

SUMMARY

The thesis contains studies of macroporous networks of oxidic materials and carbon as well as of mesoporous spheres of aluminosilicates. In what follows, a brief description of the results is given.

Ordered mesoscale hollow spheres (1000 nm diameter) of binary oxides such as TiO_2 and ZrO_2 as well as of ternary oxides such as ferroelectric $PbTiO_3$ and $Pb(ZrTi)O_3$ have been prepared by templating against colloidal crystals of polystyrene, by adopting different procedures.

Macroporous carbons of different pore sizes, containing three-dimensionally connected voids, have been prepared by an elegant method. The method involves the coating of ordered silica spheres with sucrose, followed by carbonization using sulfuric acid, and the removal of silica with aqueous hydrofluoric acid. The carbon samples show the expected optical properties. The surface area of the macroporous carbon samples varies between 120 to 550 m^2g^{-1} depending on whether non-porous or mesoporous silica spheres were used as templates.

Macroporous silica-alumina composites with mesopores have been prepared by employing polymethylmethacrylate beads as templates in the presence of the cationic surfactant, N-Cetyl-N,N,N-trimethylammonium bromide. The Si/Al ratio in

the composites has been varied between 4.5 and 48 and the occurrence of mesopores has been verified by X-ray diffraction. The surface areas of the samples vary between 676 and 1038 m^2g^{-1}, with the highest value in the sample with Si/Al = 48.0.

Mesoporous aluminosilicate spheres of 0.3 – 0.4 μm diameter, with different Si/Al ratios, have been prepared by surfactant templating. The surface area of these materials is in the 510 - 970 m^2g^{-1} range and the pore diameter in the 15-20 Å range.

---

* A paper based on a part of the work described has appeared in Solid State Sciences, 2000 **2** 877. One paper is to appear in Bull. Mater. Sci., 2001 **24** 101 and another has been submitted for publication.

1. INTRODUCTION TO POROUS MATERIALS

The design of inorganic materials with novel structures and properties has long been a prime objective of materials research. Chemists have been able to make a variety of materials based on their understanding of structure-property relations. Porous solids form a major part of materials research due to their wide range of applications: for example as membranes for separation and purification,[1] as high surface area adsorbents,[2] as solid supports for sensors and catalysts[3] and photonic band gap materials for use in optoelectronics.[4] According to their pore sizes, the International Union for Pure and Applied Chemistry (IUPAC) has recommended a specific nomenclature for porous materials: microporous (pore diameter < 2 nm), mesoporous (2 nm < pore diameter < 50 nm) and macroporous materials (pore diameter > 50 nm)[5] (Figure 1.1). These classes of porous materials are prepared by different methods and have different properties and uses.

1.1 Microporous materials

Microporous materials with three-dimensional frameworks are synthesized using molecular units or hydrated alkali or alkaline earth cations as templates. The pore structure and size in these materials are well defined. Zeolites belong to this class of porous materials. First discovered in mid-1700's, zeolites are hydrated, crystalline aluminosilicates that organize into stable, discrete frameworks.[6] Basic structures employ tetrahedral atoms (silicon or aluminium) bridged by oxygen atoms, where each oxygen

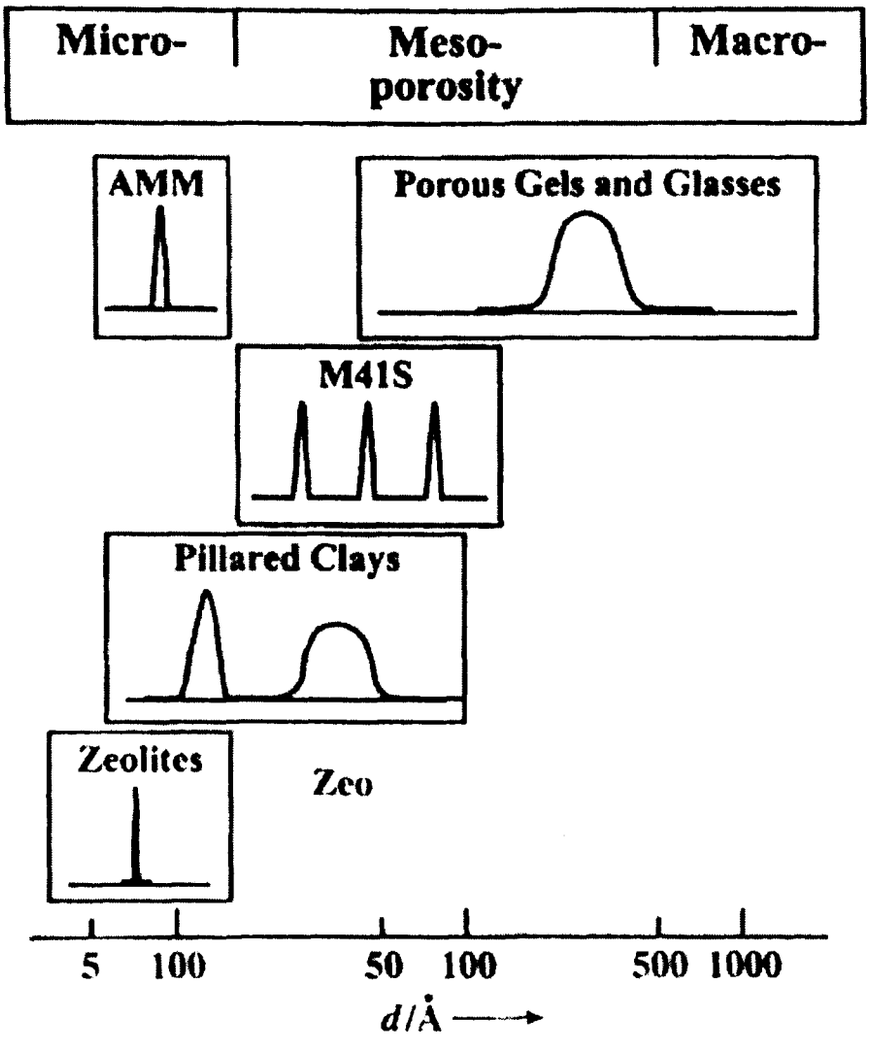

Figure 1.1. Classification of porous materials based on their pore size

atom is shared between two metalloid tetrahedra. Resulting covalent lattices can be neutral or negatively charged and often employ alkali metal or alkaline earth counterions to balance the charges. Synthetic zeolites are generally prepared hydrothermally.

More recently, compounds that exhibit similar framework structures have been synthesized in which Al and/or Si are substituted by other elements such as Be, B, Ga, Ge, Zn and P. This has given rise to a new family of microporous materials called open framework materials which use structure directing agents such as organic amines, etc. to help nucleate and direct the formation of microporous structures.[7] They find applications in the field of ion-exchange (use of Zeolite A as water softener in detergents), sorption and catalysis.

The evolution of pore sizes in microporous materials is depicted in Figure 1.2.[6]

1.2 Mesoporous materials

The limitation of pore size in microporous materials had been a matter of concern for chemists, and they were constantly exploring synthetic methods to break the pore size barrier and crossover to materials with mesoscopic dimensions having crystallinity similar to that of microporous materials. In 1992, scientists at Mobil Oil Research and Development got over this limitation by the direct synthesis of the first broad family of mesoporous solids (denoted M41S).[8,9] Three members of the M41S family were

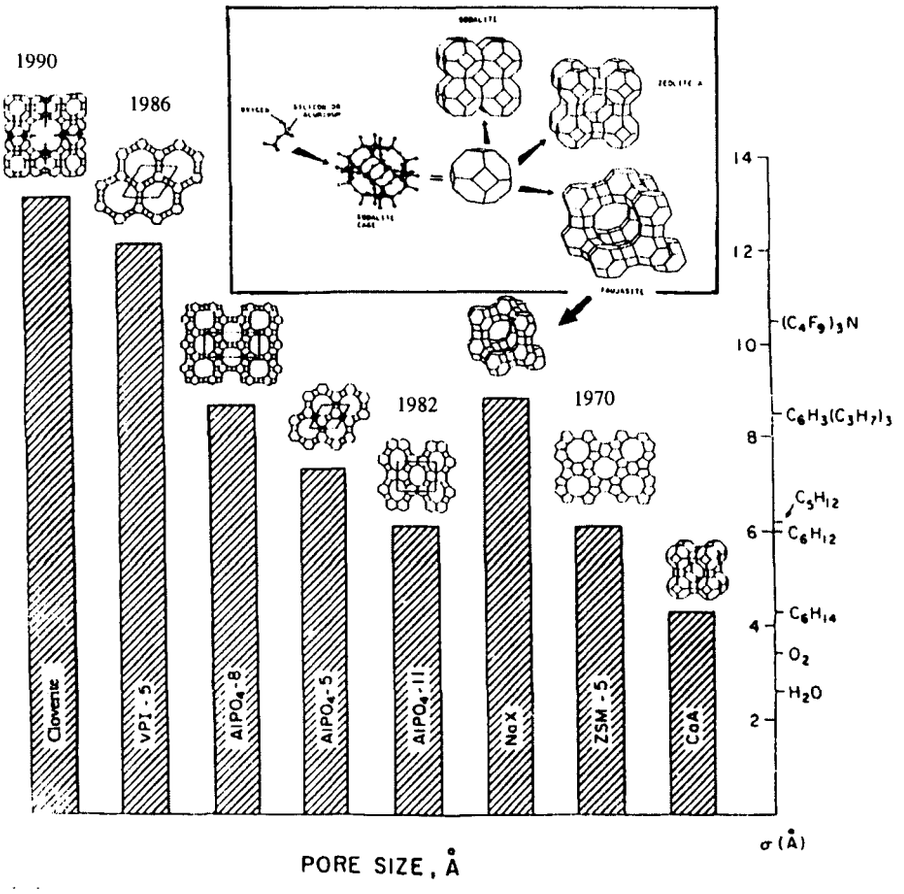

Figure 1.2. Evolution of pore size in microporous materials

distinguished: hexagonal MCM-41, cubic MCM-48 and lamellar MCM-50. There are several reviews that deal with the synthesis and characterization of mesoporous solids.[10]

Various mesoporous metal oxides such as alumina,[11] titania,[12] chromia,[13] tin oxide[14] and zirconia[15] have been prepared. Other mesoporous materials that have been synthesized include silicophosphates,[16] silicoaluminophosphates[17] and aluminophosphates.[18]

The initial reports on mesoporous materials dealt with the synthesis of new systems and in understanding their formation mechanism. Later people began trying to control the morphology of the materials and make them organize into desired shapes. Using oil/solution emulsion as templates, Schacht et. al. showed that mesoporous silica can form hollow spheres, fibres or thin sheets.[19] Ozin and co-workers described the synthesis of oriented mesoporous silica films grown on the mica-water or air-water interface.[20] They further obtained a rich diversity of morphology of mesoporous silica, namely spheres and gyroids.[21] Schaumacher et. al.[22] developed a novel synthetic method for preparing spheres of MCM-48 silicate doped with different elements like Al, Cr, V, Ga, and Nb. Using NMR they verified that the elements were indeed a part of the silica framework and not in the pores.

Formation of MCM-41 form of silica involves liquid crystalline templating. One pathway proposed by Chan et. al.[23] involves the independent organization of surfactant molecules in the form of randomly ordered rod like micelles prior to interaction with

inorganic species. Due to the charge interaction between the cationic headgroup and anionic inorganic species or between the anionic headgroup and cationic inorganic species or via hydrogen bonding between neutral amine with hydrophilic inorganic silicate, the inorganic species get attracted to the surface of the micellar rods. The second pathway proposed by Huo et. al.[24] states that the silicate anions in solution, by virtue of their charge balance with the cationic surfactant, force the surfactant molecules to form supramolecular arrays.

Mesoporous solids have very large surface areas (700 to 1200 m^2g^{-1}) and are useful as catalysts.

1.3 Macroporous materials

Several techniques have been employed to increase the pore diameter of the mesoporous materials, with a narrow pore-size distribution. These include the use of surfactants aggregated with auxiliary organic molecules,[25] by adjusting surfactant and co-cation concentrations,[26] and post-synthesis treatment of mesoporous sieves.[27] Inspite of these efforts, it was not possible to increase the pore size beyond a certain limit.

The most convenient and efficient route to synthesize macroporous materials is using the templating method.[28] The templates are colloidal spheres that are assembled into close-packed arrays. These can be highly ordered over centimeters in length. The void space is then infiltrated with precursors, which may be either organic or inorganic

depending on the template used. This forms a composite containing the template whose void space is filled with the precursor. The template is removed either by calcination of by treatment with a solvent to give macroporous materials. These solids are ordered in three dimensions and the voids are interconnected.

They find applications as supports for catalysis,[29] as filters in separation,[30] as building blocks in tissue engineering[31] and as photonic crystals.[4]

2. AN OVERVIEW OF MACROPOROUS MATERIALS

Macroporous materials contain pores with pore diameters greater than 50 nm. Such materials occur in Nature and have been put to use. These include materials such as charcoal that are macroporous carbon in the amorphous form and used as catalyst supports. It is a great challenge for materials scientists to prepare macroporous solids that contain three dimensionally ordered pores.

"Nature abhors voids", but these solids contain voids of diameters larger than 50 nm. They have over 70% air and have surface areas of several square meters. They are still sturdy enough to withstand routine handling. The voids of these samples are highly ordered over large length scales and are interconnected by small windows that give solvents and gases ready access to the internal surface. Since the porous structure is ordered and the surface is relatively flat, the materials possess striking optical properties.

2.1 Synthesis of macroporous materials

A number of methods have been developed for producing macroporous membranes including those based on selective etching (electrochemical etching of alumina or silicon,[32] chemical etching of glasses,[33] and ion-track etching of polymers[34]), those based on the self assembly of block copolymers,[35] and those based on replica moulding against various kinds of templates.[36] Methods based on the selective etching usually generate straight, one dimensional channel structures and have been very

successful in the manufacture of many commercial membrane films.[32-34] Methods based on the assembly of block copolymers are very elegant but only form arrays of spherical pores that are isolated from each other. Template-directed synthesis is a convenient and versatile method for generating porous materials. It is also a cost-effective and high-throughput procedure.

The term templating refers to a technique that involves first the formation of a temporary medium, the template, whose interstices are then filled with another material. The template is subsequently removed chemically or thermally, leaving behind a porous material that is and inverse replica of the template microstructure. The architecture and form of the resulting porous sample thus depends directly on the characteristics of the starting template. In particular, templating against opaline arrays of colloidal spheres offers a generic route to macroporous materials that exhibit precisely controlled pore sizes and highly ordered three dimensional porous structures. Figure 2.1 illustrates the schematic procedure for this approach. After the opaline array of colloidal spheres has been dried, the void spaces (~26% by volume) among the colloidal spheres are fully infiltrated with a suitable liquid precursor. Subsequent solidification of the precursor and removal of the colloidal spheres gives a three dimensional porous structure that has a highly ordered architecture of uniform air balls (interconnected to each other by small circular "windows").

The fidelity of this procedure is mainly determined by Van der Waals interaction between the templating spheres and the precursor, the wetting of the template surface,

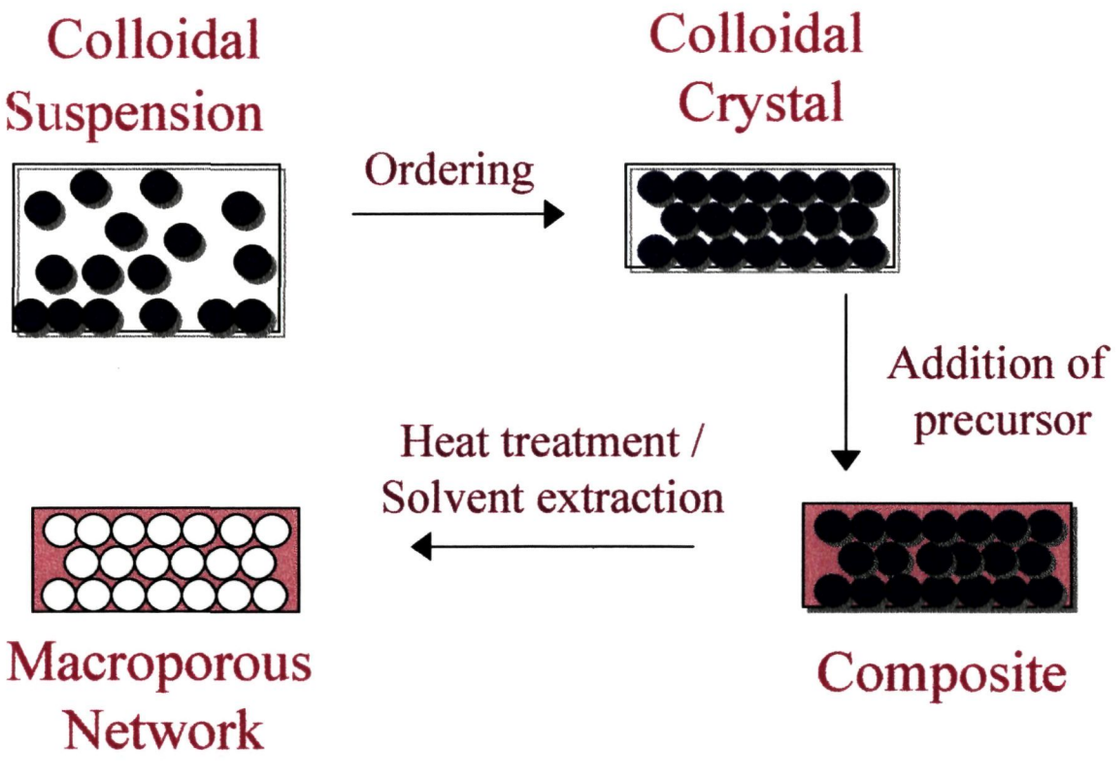

Figure 2.1. General scheme for synthesizing macroporous materials

kinetic factors such as the filling of the void spaces in the template, and the volume shrinkage of the precursors during the solidification process. The porous material obtained by this approach have also been referred to as "inverse opals" or "inverted opals" because they have an open, periodic three dimensional framework complementary to that of an opaline structure. This approach is remarkably simple and the size of the pores and the periodicity of the porous structure can be precisely controlled and readily tuned by changing the size of the colloidal spheres. The only requirement seems to be the availability of a precursor that can infiltrate into the void spaces among the colloidal spheres without the significant swelling or dissolving the template.

The templating spheres: A very important step that ensures the long-range ordering and the interconnectivity of the final porous structure is the synthesis and ordering of the templating colloidal spheres.

The templating spheres that are used are either inorganic, like silica, which is used to template organic materials like polymers[37,38] or carbon[39] or the spheres may be polymers like polystyrene (PS), which are used to make inorganic oxides[40-43] or polymethylmethacrylate (PMMA), which are used to make macroporous alloys.[44]

A wide variety of chemical approaches are available for producing colloidal spheres that are monodispersed in size.[45] The best established and most commonly used methods seems to be controlled precipitation for inorganic oxides and emulsion polymerization for polymer latex spheres, respectively. Using these methods, inorganic

oxides such as amorphous silica have been readily prepared as uniform spheres with diameters ranging from few nm to 1 μm; polymer latexes of 20 nm to 20 μm in size have also been routinely produced as uniform beads.

Inorganic colloids are usually prepared via precipitation reactions, a process that often involves two sequential steps: nucleation and growth of the nuclei. To achieve monodispersity, these two stages must be strictly separated and nucleation should be avoided during the period of growth. In a closed system, the monomer (usually exists as a complex or solid precursor) must be added or released slowly at a well-controlled rate in order to keep it from passing the critical supersaturation levels during the growth period. In 1968, Stöber and Fink applied this strategy to other systems and demonstrated an extremely useful procedure for preparing monodisperse silica colloids.[46] They hydrolyzed a dilute solution of tetraethylorthosilicate (TEOS) in ethanol at a high pH and obtained uniform spheres of amorphous silica whose sizes could be varied from 50 nm to 2 μm simply by changing the concentration of the reactants. This method was later improved by many others, and now seems to be the simplest and most effective route to monodisperse silica spheres.[47] Mccomb and coworkers have studied the effect of varying the various parameters such as the concentration of the base and obtained results that were fairly reproducible.[48] As a general rule, it is necessary to precisely control the reaction conditions – for example, the temperature, the pH, the method for mixing of reactants, the concentration of the reactants, and the concentration of the counterions – to generate a single, short burst of nuclei and the let these nuclei grow uniformly. Silica colloids represent one of the best-characterized inorganic systems that have been

manufactured as monodisperse samples, as well as in large quantities. The surface of the as-synthesized silica colloids is often terminated with silanol groups (-Si-OH), which can ionize to generate a negatively charged interface at pH values higher than 7.[47] Pristine samples of silica colloids will undergo a series of changes when they are thermally treated at elevated temperatures. The absorbed water (~5 wt.-%) will be released first at ~150 °C; the silanol groups will be crosslinked via dehydration in the temperature range of 400-700 °C; and these particles will start to fuse into aggregates when the temperature is raised above the glass transition temperature of amorphous silica (~800 °C).

Polymer colloids of different chemical compositions can be produced as exceedingly uniform spheres by a process called emulsion polymerization.[49] The major components of this process include a monomer, a dispersion medium (in most cases, water), an emulsifier (surfactant), and an initiator (usually water soluble). The monomer is dispersed as an aqueous emulsion (~1-100 μm) with the help of the emulsifier. According to the proposed mechanism, most surfactant molecules exist as micelles (~10 nm in diameter), and the majority of these micelles have been swollen by the monomer. The formation of polymer latexes begins with the decomposition of the water-soluble initiator during which a burst or primary free radicals are generated. These radicals polymerize the small amount of monomer that is dissolved in the aqueous phase to form the nuclei-oligomers in the form of tiny particles. These nuclei subsequently enter the micelles and eventually grow into larger particles until all the monomer dissolved in each micelle has been consumed. At the same time, the monomer encapsulated in the emulsion droplets act as reservoir to provide a supply of repeating units to the growing polymer

chains through diffusion. The growth of polymer latexes will stop at the point when all the monomer has been depleted.[49] For a polymer latex that is 100 nm in size, there are approximately 1000 macromolecular chains entangled as coils in the sphere; each chain starts and ends with a functional group formed by the decomposition of the radical initiator. Monodispersed polymer colloids such as PMMA and PS have been produced in large quantities by using this technique.[49]

Formation of Colloidal Crystals: There are many ways in which the templating colloidal spheres can be ordered into three-dimensional arrays. Figure 2.2 illustrates two methods using which colloidal spheres have been successfully assembled into arrays.

Sedimentation in a gravitational field (Figure 2.2A) seems to be the simplest approach to the formation of 3D crystalline spheres from colloidal spheres.[50] Even though it looks simple, this method involves a strong coupling of several complex processes such as gravity settling, translational diffusion (or Brownian motion), and crystallization (nucleation and growth). The parameters that we must control in order to get good crystals are the size and density of the colloidal spheres, as well as the rate of sedimentation. The spheres will always settle completely to the bottom of the container as long as the size and density of the spheres is sufficiently high. Only when the sedimentation process is slow enough, the colloidal spheres concentrated at the bottom will undergo a hard-sphere disorder-to-order phase transition to form a three-dimensionally ordered lattice. If the parameters are not adjusted rightly, then the spheres will remain dispersed in the medium.

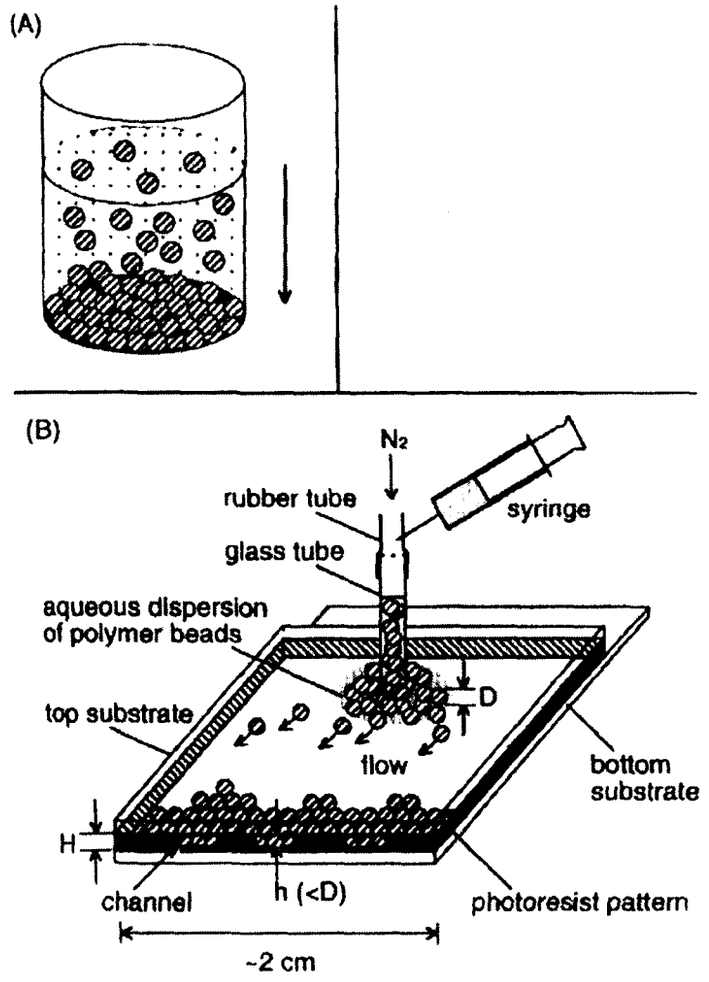

Figure 2.2. Methods used to assemble colloidal spheres into 3D lattices: A)Sedimentation and B)Crystallization through physical confinement.

Silica spheres have been successfully used to make 3D ordered arrays using this method to form artificial or synthetic opals.[51,52] It is generally accepted that the 3D crystalline arrays produced by this method have cubic-close-packed (ccp) structure rather than a hexagonal-close-packed (hcp) structure. Recently Colvin and co-workers developed a layer-by-layer sedimentation for fabricating ccp arrays of silica colloids.[51]

The major disadvantage of this method is that it has very little control over the morphology of the top surface and the number of layers in the array.[53] It also takes relatively long periods of time, from weeks to months, for sub-micrometer sized spheres. The 3D arrays produced by this method are polycrystalline in nature. Inspite of these, due to the relatively low costs involved and the simplicity of the method makes it a widely used technique.

Monodisperse colloidal spheres often organize themselves into a highly ordered 3D structure when they are subjected to a physical confinement.[54] Xia and co-workers recently demonstrated such a method, which is schematically shown Figure 2.2B. Using this method, they were able to assemble spheres with diameters ranging from 50 nm to 1 μm. The 3D crystalline array was found to be ccp structure with a packing density very close to 74 %, and the (111) face was parallel to the glass substrate. They were able to assemble polystyrene as well as silica colloids to get 3D ordering that extended into the centimeter scale.[55]

Synthesis of macroporous networks: Macroporous networks of various materials have been synthesized using colloidal crystals as templates. These include different oxides,[40-43] polymer membranes,[37,38] carbon,[39] silicon,[56] alloys,[44] and metals.[57,58]

Polymer templates, like PMMA of PS, are generally used for the synthesis of oxides. Valev et. al. used polystyrene latex microspheres of diameters ranging from 200 – 1000 nm that were soaked in the surfactant hexadecyltrimethyl ammonium bromide. These were treated with a silica solution that permeated the cavities and polymerized. The polymer spheres were removed by calcination to give networks that contained long range ordering. Vos and co-workers prepared networks of titania by a similar procedure without the use of the surfactant.[40] Stein and coworkers prepared inorganic oxide networks of Si, Ti, Zr, Al, W, Fe, Sb and a Zr/Y mixture.[42] They followed a simple and cost – effective technique in which alkoxides were used as precursors, which, in same cases had to be diluted with alcohols in order to slow down the rate of hydrolysis. They also prepared networks of aluminophosphates and hybrid organosilanes, as well as silicates with bimodal distribution of meso- and macropores. The products consisted of periodic, interconnected networks of monodisperse submicron pores extending over hundreds of micrometers. The templates were removed either by calcination (mainly for organic templates) or by solvent extraction using a tetrahydrofuran / acetone mixture (for both organic and inorganic templates). Thus, this very efficient process, subject to the availability of the alkoxide precursor, could synthesize a wide variety of oxides.

Macroporous networks of different metals have been made by different methods.[57,58] In one process, solution of gold nanoparticles were drawn into the interstices of the colloidal crystal and dried. The template was removed from this composite to give macroporous gold.[58] In another approach, nanocrystalline gold at low concentrations is used as a catalyst in an electroless plating process that can produce many types of porous metals such as nickel, cobalt, copper, silver, gold and platinum.[57]

Three-dimensionally ordered macroporous metal alloys of Ni_xCo_{1-x} (a solid solution) and Mn_3Co_7 (an intermetallic compound) have been prepared by templated precipitation of mixed metal salts within colloidal crystals of PMMA spheres and subsequent conversion of the inorganic precursors.[44] Stein and co-workers preferred the use of PMMA spheres as compared to PS spheres due to its thermal degradation character. PMMA decomposes by chain depolymerization, resulting in a gradual reduction in the molecular weight and production of the monomer. As a result, milder conditions are required to remove the template. Also, due to their increased wettability, PMMA spheres offer better penetration of the precursor.

Porous membranes of polymers have been fabricated by Xia and coworkers.[37,38] Polystyrene and silica spheres were used as templates and were ordered into arrays by the method of physical confinement that was described earlier. U-V curable polymer precursors like poly(acrylate-methacrylate) copolymer were used. The templates were removed by treatment with suitable solvent (aqueous HF for silica spheres and toluene for polystyrene spheres). The networks that were obtained were interconnected by

circular windows. Colvin and coworkers also prepared macroporous films by templating silica films with polymer precursors like methyl methacrylate, styrene, etc. and studied the optical properties if the iridescent samples.[59]

Porous carbons with 3D periodicity were prepared by using silica spheres as templates.[38] They were ordered into arrays by the sedimentation process. The ordered arrays were treated with phenolic resin after which silica was removed by treatment with aqueous HF solution to give carbon inverse opal structures. Carbon networks were also prepared using the technique of chemical vapour deposition (CVD). The silica templates were also treated with vapours of propylene and nitrogen at 800 °C for 6 hours. In this case too the template was removed by treatment with aqueous HF solution. The products obtained were iridescent in both the cases as shown in Figure 2.3. Also shown is the Scanning Electron Microscopy (SEM) image of the sample showing ordered carbon networks. Raman studies and conductivity measurements were also performed.

Silicon photonic crystals with complete three-dimensional bandgap near 1.5 μm was produced by growing silicon inside the voids of an opal template of closely-packed silica spheres followed by the removal of the silica spheres.[56] The reflectance spectrum clearly indicates the bandgap at a wavelength of 1.5 μm which is also the wavelength used by for the fibre optic telecommunication.

Synthesis of macroporous materials with dual types of pores: Materials with bimodal pore systems are of considerable interest for applications in catalysis and separations

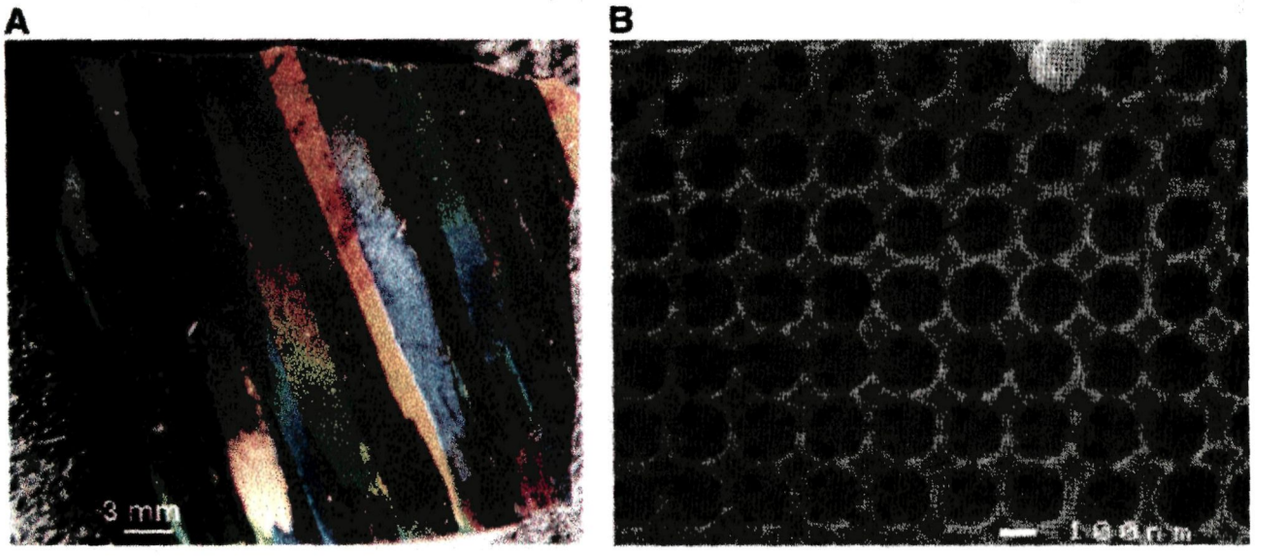

Figure 2.3. Inverse opal of carbon produced by CVD process.(A)Photograph showing opalascence (B)SEM image of a fracture surface

since they combine the benefits of each pore size regime. Stein and coworkers demonstrated the synthesis of macroporous silica containing mesoporous walls.[42] An aqueous mixture containing cetyltrimethylammonium hydroxide, TEOS and tetrapropylammonium hydroxide (TPAOH) was stirred and allowed to permeate an ordered array of PS spheres. The product was dried and calcined to get macroporous silica, whose morphology was confirmed by SEM. X-ray diffraction and adsorption studies using nitrogen gas confirmed the mesoporous nature of the walls.

Antonietti and coworkers[60] employed polymer latex spheres with different surfactant functionalities and treated them with tetramethylorthosilcate at a pH of 2. The spheres were removed from the dried composite to give systems with a bimodal pore size, though the macropores were not well ordered.

Macroporous silicates with zeolitic microporous frameworks were made hydrothermally by Stein and coworkers.[61] Ordered PS spheres was treated with TEOS and TPAOH. This was hardened to form a composite that was heated in a Teflon-lined autoclave at 130 °C. Calcination resulted in the removal of the template. X-ray diffraction and NMR verified that the walls were indeed of silicalite. SEM could not show the interconnectivity of the macropores. Nitrogen adsorption showed typical Type I characteristics of microporous materials.

2.2 Applications as photonic crystals

Due to their long-range ordering, three-dimensionally periodic macroporous structures are promising candidates for photonic bandgap applications. A photonic band gap crystal (or photonic crystal) is a spatially periodic structure fabricated from materials having different dielectric constants.[62] These materials affect the properties of photons, in much the same way that ordinary semiconductor crystals affect the properties of electrons. We see many examples of these in Nature – the bright colours of opals is due to closely packed silica spheres and the bright colours of a butterfly's wings are also due to this phenomenon. These ideas had been proposed independently by John[63] and Yablonovitch[64] in 1987 and since then have opened up a new, exciting field of research.

In a semiconductor, the atomic lattice presents a periodic potential to an electron propagating through the crystal. Due to the geometry of the lattice and the strength of the potential, Bragg-like diffraction occurs from the atoms, that opens up a gap in the allowed energy levels for which an electron is forbidden to propagate in any direction. In a photonic crystal, the periodic "potential" is due to a lattice of macroscopic dielectric media instead of atoms. If the dielectric constants of the constituent media are different enough, Bragg scattering of the dielectric interfaces can provide many of the same phenomena for photons as an atomic potential does for electrons. The aim is to produce photonic structures with a bandgap that extends over the entire Brillouin Zone - a range of frequencies for which light is forbidden to exist within the crystal. Creating a defect in the periodicity is also used to our advantage – a point defect could act as a microcavity, a line defect as a waveguide and a planar defect as a perfect mirror. Thus, it should be

possible to fabricate materials that can guide light along narrow channels and tight corners with as little loss in power as possible.

The periodic array of atoms occurs naturally in crystals but these photonic crystals need to be fabricated artificially. It should be noted that the lattice constant in these photonic crystals should be comparable to the wavelength of light. For the optoelectronic industry, where the operating frequency used is 1.5 μm, the lattice constant of a photonic crystal should be of the order of 0.5 μm.

From a theoretical point of view, the description of light in a photonic crystal must involve the solution of Maxwell's equations in a periodic dielectric medium. The advantage of Maxwell's equations is that unlike the complex strongly interacting many-particle problem of an electron in a solid, they can be solved exactly. Also, there is no fundamental length scale. That is, we could scale the solution to any length scale and obtain the same band structure. These theoretical studies help in the design and synthesis of photonic crystals.

Yablonovitch in fabricated the first three-dimensional photonic crystal possessing a complete bandgap in 1991 in the microwave regime.[65] This involved the covering a slab of dielectric with a mask consisting of a triangular array of holes. Each hole was then drilled three times along the (110)-type direction. Since then, several other 3D photonic crystal designs have appeared that offer complete bandgap.[66-69] It is difficult to apply conventional microlithography to the fabrication of 3D periodic structures with lattice

parameters comparable to visible region wavelength. The other possible techniques are based on self-assembly of monodisperse colloids[70] and template directed synthesis.[71-73] Yablonovitch has reported that a cubic close packed (ccp) array of silica spheres is the structure most likely to result in a complete bandgap.[74] This was based on the observation that the Brillouin zone of a face centered cubic (fcc) unit cell is closest to the spherical symmetry required to ensure overlap of the bandgap in all reciprocal space directions. However, other workers have suggested that the difference between fcc and hexagonal packing cubic (hcp) structures is rather small.[75] Calculations suggest that a ccp lattice is more energetically favourable[76] and experiments support this conclusion.[77,78]

A typical experiment involves the passing of white light through a photonic crystal and recording the intensity of the transmitted light. The modified Bragg's law that is applied to photonic systems is given by[79]

$$\lambda = 2d(n^2 - \sin^2\theta)^{1/2}$$

where λ is the position of the stop band, d is the interplanar spacing, n is effective refractive index and θ is the angle measured from the normal to the planes. The inter-planar spacing d can be expressed in terms of the unit cell parameter a, and the Miller indices: $d=a/(h^2+k^2+l^2)^{1/2}$. For the fcc lattice, the diameter of the spheres D is related to the lattice parameter by $a=2^{1/2}D$. Thus, knowing the position of the stop band, the effective refractive index of the medium can be calculated.

Several groups have tried to make photonic crystals of different colloids assembled into array and measured their optical properties. Colvin and coworkers[80]

investigated the photonic properties of artificial opals. They have also measured the dependence of the stop band attenuation on the number of layers along the [111] direction. Xia and coworkers[81] studied the photonic properties of opaline structures assembled from PS beads. The position of the stop band could be shifted by changing the size of the colloid particles. The studies are consistent with the computational results: there exists a pseudo bandgap for any fcc lattice self-assembled from monodisperse colloidal spheres.

Colloidal systems do not have a high effective refractive index and hence are not good candidates to exhibit full bandgap. Inverse opal structures are ideal for this purpose. The synthesis of such structures has been dealt with earlier. The most promising candidates for the matrix are titania, CdS, CdSe, etc. that have a high refractive index (greater than 2.5). Vos and co-workers[40] have demonstrated the fabrication with polycrystalline titania (anatase) by using a sol-gel process and also measured the reflectance spectrum of this crystal. Baughman and co-workers have incorporated chemical vapour deposition (CVD) to this procedure and generated inverse opals containing different forms of carbon.[39] Norris and co-workers and Braun and Wiltzuis were able to obtain 3D periodic structures from II-VI semiconductors such as CdS and CdSe, albeit no optical measurements were performed.[82,83] Stein and co-workers, Velev et. al., and Colvin and co-workers also fabricated highly ordered 3D porous materials from metals that might display interesting photonic properties.[41,42,57] Pine and co-workers[84] and Subramania et. al.[73] have fabricated inverse opals of titania by filing the void spaces among colloidal spheres with slurries of nanometer-sized titania particles.

Despite these advances, a definite signature of a complete photonic bandgap was still missing for these 3D porous materials. Recently, Blance et. al. reported the synthesis of silicon photonic crystals with a complete three-dimensional bandgap near 1.5 μm.[56] The reflectance spectrum that they recorded clearly verified this.

All the photonic properties are technologically important because they can be exploited, in principle, to produce light-emitting diodes (LEDs) that display coherence properties, to fabricate thresholdess semiconductor diode lasers, and to significantly enhance the performance of many other types of optical, electro-optical, and quantum electronic devices. The future research will be directed at producing different materials possessing 3D photonic bandgap, which can be manufactured cost-effectively and in a large scale.

2.3 Concluding Remarks

Other types applications of macroporous materials that have been proposed include their potential usage as collectors of solar energies, as model systems for studying quantum confinement, as electrodes for fuel cells and other types of electrochemical processes, as supports for catalysis, and as low-dielectric materials for capacitors. A brief description of photonic crystals is given below. The past few years has witnessed a tremendous surge of interest in macroporous materials. The methods to synthesize these materials were the focus of most of the work being done hitherto. Future research would be aimed at the use of these materials in the applications that have been proposed.

3. SCOPE OF THE PRESENT INVESTIGATIONS

In what follows, the scope of investigations reported in this thesis is presented.

3.1 Macroporous oxide materials with three-dimensionally interconnected pores.

Macroporous networks of various oxides have been synthesized using spheres of polystyrene or PMMA as templates. Velev et. al.[41] obtained ordered macroporous silica by templating colloidal crystals of polystyrene while Imhof and Pine[43] obtained macroporous titania by using surfactants. The preparation of a few ceramic oxides with periodic three-dimensional arrays of macropores by using polystyrene spheres as templates has been reported.[28,37,42] Macroporous TiO_2 with diameters between 240 and 2000 nm has also been prepared by filling voids in opals by a liquid phase chemical reaction.[40] While some of the workers have removed the organic template by dissolution in an appropriate solvent,[37] others have burnt off the polymer template[43] or extracted it by refluxing in a solvent.[37,42]

In our study, we have prepared ordered mesoscale hollow spheres of ~1000nm diameter of binary as well as ternary oxides by employing crystalline arrays of polystyrene beads as templates. Typical of the ordered macroporous ternary oxides obtained by us is ferroelectric $PbTiO_3$ and $Pb(ZrTi)O_3$. In preparing these ordered porous networks, we have employed calcination as well as washing with a solvent as the means of removing the template.

3.2 Macroporous carbons obtained by templating with silica spheres.

Macroporous membranes of various polymers have been prepared by templating silica spheres.[38] Porous carbons with similar features have been prepared by infiltering silica opal plates with a phenolic resin or by chemical vapor deposition using propylene, and then dissolving the silica.[39] We have prepared macroporous carbon with three dimensionally interconnected voids by a novel method, involving the coating of close-packed monodisperse silica spheres with sucrose, converting sucrose into carbon by mild carbonization using sulfuric acid as the catalyst,[85] and then dissolving the silica with aqueous hydrofluoric acid. In this article, we wish to draw attention to the excellent results obtained by this technique in preparing three-dimensionally ordered macroporous carbon networks. We have also prepared carbon samples with macropores by using mesoporous silica spheres instead of the non-porous silica spheres. We also present the adsorptive properties of the various macroporous carbon samples prepared by us.

3.3 Macroporous silica-alumina composites with mesoporous walls.

Macroporous materials of oxides such as TiO_2, SiO_2[40-43] are attracting much attention. Macroporous solids with micropores or mesopores would make useful adsorbents or catalyst supports. Recently, Stein and coworkers have reported the synthesis of macroporous silica containing mesoporous walls by treating a solution containing the silica precursor with an aqueous mixture of cetyltrimethylammonium hydroxide and tetrapropylammonium hydroxide and pouring the solution over an ordered array of polystyrene beads.[42] Macroporous silicates with zeolitic microporous

frameworks were made hydrothermally by Stein and coworkers.[61] We have attempted to make macroporous aluminosilicates containing mesoporous walls. For this purpose we have employed an ordered array of polymethylmethacrylate spheres in the presence of the cationic surfactant N-Cetyl-N,N,N-trimethylammonium bromide (CTAB). We describe the macroporous-mesoporous silica-alumina composites with satisfactory/high surface areas.

3.4 Submicron-sized mesoporous aluminosilicate spheres.

The discovery of mesoporous silica marks a major event in areas related to catalysis, sorption and separation processes.[8,9] Amongst the criteria for the use of such mesoporous materials for various purposes, the morphology and particle size are important ones. In this context, several workers have attempted to prepare sub-micron sized mesoporous silica spheres. The synthetic procedure generally makes use of Stöber's reaction involving base hydrolysis and subsequent condensation of the silicon ester in an appropriate solvent.[46] One of the first efforts to make spherical silica is due to Unger et al,[86] who obtained non-porous silica beads with a particle size of ~3 μm. Kaiser and Unger,[87] however, obtained completely porous silica spheres by a similar procedure. Büchel et. al.[88] have described a novel pathway for obtaining monodisperse silica spheres composed of a non-porous solid silica core and a thin mesoporous silica shell by taking advantage of the methods described by Unger et. al.[86] and Kaiser and Unger.[87] By employing surfactant-stabilized emulsions as in the synthesis of MCM-41, Huo et. al.[89] obtained large, monodisperse mesoporous silica spheres with high surface areas. The spheres had diameters between 0.1 to 2 mm and pore diameters of 1 to 5 nm. Mesoporous silica spheres ranging from 2 to 6 μm (pore

diameter ~2.5 nm) have been synthesized under static acidic conditions by mixed cationic-nonionic surfactant templating as well.[90] Spheres of ordered MCM-41 and MCM-48 have also been prepared by employing appropriate surfactants.[22,91] It was our interest to prepare monodisperse aluminosilicate spheres with mesoporous properties. We have been able to prepare such spherical aluminosilicates with Si/Al ratios between 14 and 40 by employing a cationic surfactant. For purpose of comparison, we have also prepared mesoporous silica spheres by the same procedure.

4. EXPERIMENTAL

4.1 Macroporous oxide networks

Polystyrene beads of 1000 nm diameter, prepared by emulsifier-free polymerization of styrene, were centrifuged at 1100 rpm for six hours and dried in air. These beads yielded satisfactory colloidal crystals, as can be seen from a scanning electron microscopy (SEM) image (obtained with a Leica microscope) of a dispersion shown in Figure 4.1. We prepared macroporous networks of SiO_2, TiO_2 and ZrO_2 by using tetraethylorthosilicate (TEOS), tetrabutylorthotitanate (TBOT) and zirconium i-propoxide (ZIP) respectively as the precursors. Macroporous SiO_2, TiO_2 and ZrO_2 networks were prepared from using alkoxide precursors by the following procedure - Polystyrene spheres were taken on a Büchner funnel connected to a vacuum pump. The ratio of the weights of the metal precursors (TEOS, TBOT, ZIP) to the template was 10.0, 5.0 and 2.5 for SiO_2, TiO_2 and ZrO_2 respectively. The pure precursors were poured on the template to wet it completely. The precursors hydrolyzed on exposure to air. The composites were left to dry for 12 hours at room temperature. The template was removed by calcination at 575^0C for 7 hours.

Macroporous TiO_2 was prepared by an alternative route as well. $TiCl_4$ was taken in a 3-necked round bottom flask and kept in salt-ice mixture. Distilled water ice pieces were added to it slowly to form a yellow coloured solution. Distilled water was finally added to get a transparent solution. This was poured on polystyrene beads kept in a glass

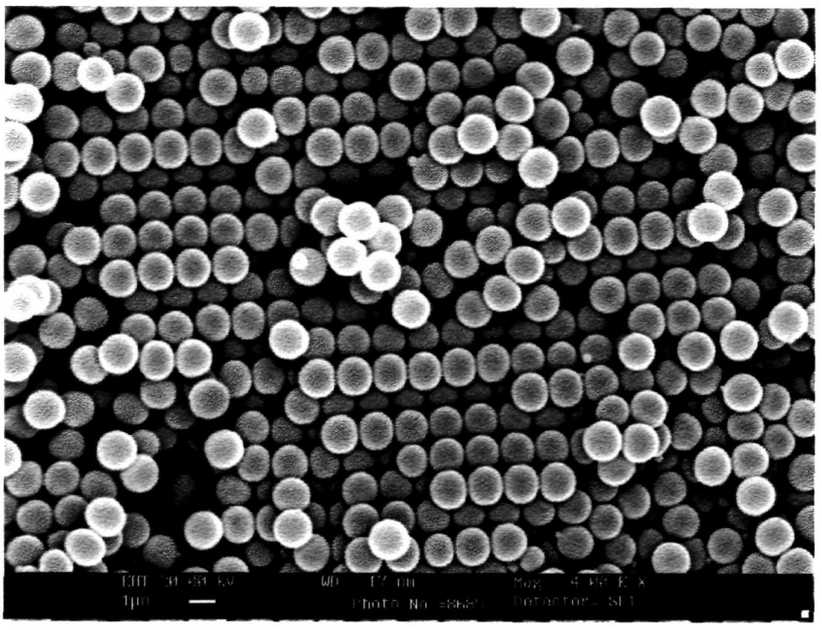

Figure 4.1. SEM image of an array of polystyrene beads

vial and allowed to dry at room temperature. The template was removed by treatment with toluene.

Macroporous $PbTiO_3$ and $Pb(ZrTi)O_3$ (PZT) were prepared by the following procedure - 0.1M solution of lead acetate, 0.1M TBOT and 0.1M ZIP (all in methanol) were prepared. In order to prepare $PbTiO_3$, stoichiometric amounts of the Pb and Ti precursor solutions were taken in a beaker. The solution was stirred for 15 minutes after which it the temperature was increased to 60°C. A few drops of water were added to the solution, which resulting in gel. This was poured on the polystyrene spheres and allowed to dry at room temperature for 12 hours. The template was removed by treatment with toluene. The sample was crystallized by heating to 400^0C for 60 minutes. $Pb(Zr_{0.5},Ti_{0.5})O_3$ was obtained by a similar procedure (starting with Pb, Zr, Ti precursor solutions).

X-ray diffraction (XRD) of the products was recorded. Scanning Electron Microscopy (SEM) was carried out on all the samples to study their morphology.

4.2 Macroporous carbon networks

The procedure employed by us for the synthesis of macroporous carbon is as follows. Monodisperse silica spheres were synthesized following the method of Stöber et al.[46] Spheres of different sizes could be prepared by the hydrolysis of

tetraethylorthosilicate (TEOS) in an alcohol medium with aqueous ammonia (25% solution) as the base. Evaporation of the alcohol solvent from between the spheres packs them into arrays. In Figure 4.2 (a) and (b) we show a SEM image of ordered silica beads of diameter ~625 and ~200 nm respectively. The spheres have a narrow size distribution and are reasonably ordered. In order to template the silica spheres with carbon, 0.245g of the spheres was treated with a solution containing 0.2g sucrose along with 4 mL H_2O and 0.5 mL H_2SO_4. The resulting mixture was kept in a drying oven at 60°C for 6 hours, and the temperature gradually raised to 100°C to allow complete drying. The temperature was then increased to 150°C at a rate of 2 °/min. Carbonization was carried out by heating the sample to 800°C under vacuum (10^{-6} Torr). The composite thus formed was treated with an aqueous solution of HF (48%) for 24 hours in order to dissolve the templating silica spheres. Aqueous HF was found to be better than aqueous NaOH for the dissolution. The product was washed several times with water and dried at 60°C. Macroporous carbon samples were prepared by this procedure by employing non-porous silica spheres of diameters ~625 and ~200nm.

We also prepared macroporous carbon by templating mesoporous silica spheres with sucrose. For this purpose, monodisperse silica spheres containing mesopores (diameter ~450 nm) were prepared by a method similar to Schumacher et al.[22] In a typical synthesis, 0.667g of N-cetyl-N,N,N-tetramethylammonium bromide was dissolved in a solution containing 14 mL H_2O and 14 mL C_2H_5OH. To the above solution, 3.5 mL ammonia (25% solution) was added under stirring. After 10 minutes, 1 mL of TEOS was added dropwise and stirred for a period of 2 hours. The mixture was aged at room

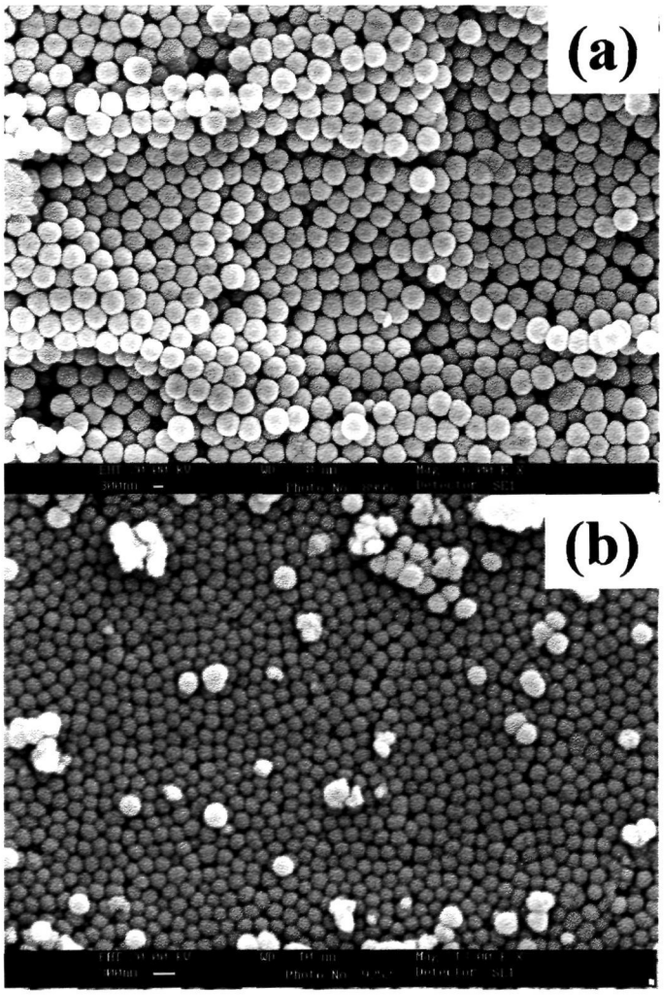

Figure 4.2. (a)SEM image of non-porous ordered silica spheres of ~625 nm diameter. (b) SEM image of non-porous, ordered silica spheres of ~200 nm diameter.

temperature (25°C) for 2 hours, filtered, washed with deionized water and dried at ambient temperature. The dried product was calcined at 400°C for 2 hours. Powder XRD patterns that was recorded established the mesoporous nature of the sample. Thermogravimetric analysis (TGA) showed that ~95% of the surfactant could be removed by calcination at 400°C. SEM images showed the particles to be spherical, but there was a distribution of sizes. These spheres were taken along with water and sonicated for 30 minutes in order to disperse the spheres. This was left undisturbed at room temperature until a major part of the water had evaporated. The rest of the water was then evaporated at 60°C. In Figure 4.3(a) we show an SEM image of the mesoporous silica spheres. Due to the variation in the sizes of the spheres, it was found difficult to order them into arrays. Using these spheres, macroporous carbon networks were prepared by a procedure similar to the one used for templating the non-porous silica spheres.

We also employed an array of silica spheres containing 25% mesoporous spheres (~450 nm diameter) and 75% non-porous spheres (~625 nm diameter) for preparing porous carbon samples. This was done by taking the spheres in water, followed by sonicating for 30 minutes. The spheres settled down under the influence of gravity. The SEM image of the dried spheres is shown in Figure 4.3(b). The ordering is considerably improved due to the presence of a larger percentage of uniform sized non-porous spheres. Employing these arrays, we repeated the synthesis of macroporous carbon.

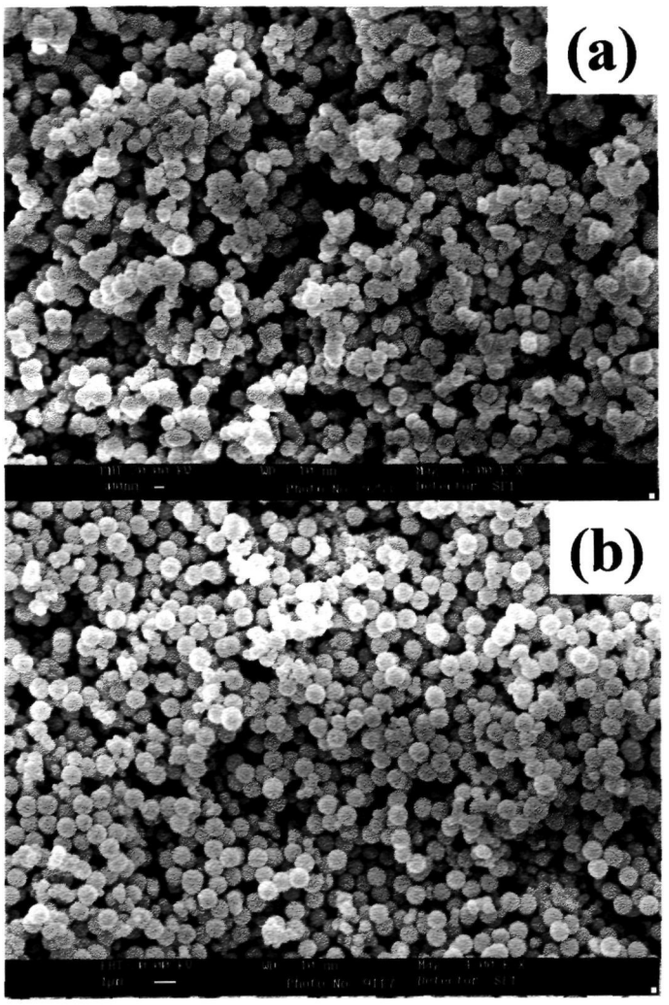

Figure 4.3. (a)SEM image of mesoporous silica spheres of ~450 nm diameter. (b) SEM image of a mixture of mesoporous (25%) and non-porous (75%) silica spheres.

The application of porous carbons as catalyst supports is widely recognized and we therefore carried out nitrogen adsorption studies at liquid nitrogen temperature on these samples. Reflectance spectra of the macroporous carbons were recorded in the visible region for the samples prepared with non-porous silica spheres (~200 nm diameter).

4.3 Macroporous silica-alumina composites with mesoporous walls

Polymethylmethacrylate (PMMA) spheres of diameter 275 nm were obtained from Soken Chemicals, Japan. These were taken as 1 % wt:wt in distilled water and sonicated for 30 minutes to disperse the spheres. This sol was centrifuged at 1000 rpm for 6-8 hours. The water above the spheres was removed with a pipette carefully and the spheres were left to dry under ambient conditions. These formed millimeter-sized colloidal crystals which were used for further reactions.

The silica-alumina gel was synthesized in the following manner. To a solution of 0.5g of CTAB in 10 mL H_2O, 0.1g of $Al_2(SO_4)_3.16H_2O$ was added and stirred until a homogenous solution was obtained. 1 mL of tetraethylorthosilicate (TEOS) was added to this mixture and the stirring continued. Finally, a few drops of NH_3 (25% solution) were added to make the pH ~8. The turbid solution was poured on the colloidal crystals to allow it to percolate through the voids between the spheres. This was left to dry at room temperature. The dried products were calcined at 400°C for 2 hours, which resulted in sample A shown in Table 1. By a similar procedure, we prepared two other silica-alumina samples (B and C) with different Si/Al ratios.

Powder XRD patterns of the samples were obtained to confirm the nature of the mesophase. TGA was carried out to get the amount of template removed on calcination. SEM and energy-dispersive X-ray (EDX) analysis were carried out to analyze the composition of the samples. Nitrogen adsorption studies were carried out at liquid nitrogen temperature on these samples in order to get the surface area and the nature of the pores. Solid state MAS NMR measurements were performed to obtain the co-ordination of Al and Si.

4.4 Mesoporous aluminosilicate spheres

We have prepared mesoporous aluminosilicate spheres with Si/Al ratios in the range 14 to 40 in addition to preparing pure silica mesoporous spheres by the following procedure. In a typical synthesis, 0.667g N-cetyl-N,N,N-trimethylammonium bromide (CTAB) was dissolved in a solution containing 14 mL deionised water (H_2O) and 14 mL ethanol (C_2H_5OH). To the above solution, 3.5 mL ammonia (NH_3) solution (25%) was added under stirring, followed by the addition of a solution of 15 mL water of an aqueous solution containing 0.1g $Al_2(SO_4)_3$. The final composition of the mixture was 0.4MCTAB/360M H_2O/53MC_2H_5OH/41.76MNH_3/1MTEOS/0.0355M$Al_2(SO_4)_3$. After 10 min, 1mL of tetraethylorthosilicate (TEOS) was added dropwise over a period of 2h under stirring to obtain a gel. The gel was aged at room temperature (298 K) for 16h, filtered, washed with deionised water and dried at ambient temperature. The dried product was calcined at 200°C for 4h, which resulted in sample C. By a similar

procedure, we prepared two other aluminosilicate samples (A and B) with different Si/Al ratios. Powder XRD patterns of the samples were obtained to determine if the samples were mesoporous. TGA was carried out to get the amount of template removed after calcination. SEM and energy-dispersive X-ray (EDX) analysis were carried out to observe the morphology and analyze the composition. Nitrogen adsorption studies were carried out at liquid nitrogen temperature on these samples in order to get the surface area and the nature of the pores. Solid state MAS NMR measurements were performed to obtain the co-ordination of Al and Si.

4.5 Characterization techniques

Powder X-ray diffraction (XRD) patterns were recorded using CuKα radiation on a Rich-Siefert, XRD–3000-TT diffractometer. The Thermogravimetric analysis (TGA) of the samples was carried out on a Mettler-Toledo-TG-850 instrument. Energy dispersive analysis of X-rays (EDAX) and Scanning Electron Microscopy (SEM) images were obtained on a Leica scanning electron microscope fitted with a Link ISIS spectrometer. Surface areas and adsorption isotherm of the samples were measured using the Brunauer-Emmett-Teller (BET) method with the help of the adsorption setup fitted with a Cahn-2000 microbalance. Magic angle spinning nuclear magnetic resonance (MAS-NMR) were recorded on a Bruker DX-300 spectrometer.

5. RESULTS AND DISCUSSION

5.1 Macroporous oxide materials with three-dimensionally interconnected pores.

In Figure 5.1(a) we show the SEM image of the ordered macroporous SiO_2. The pore diameter is slightly smaller (~850 nm) than that of the template beads because of shrinkage occurring during calcination. What is interesting is that we see lower layers in the SEM image due to the three-dimensional ordering in the material, although it is X-ray amorphous.

The SEM image of macroporous TiO_2 prepared by the TBOT route is shown in Figure 5.2(a). The pores are highly ordered and there is some shrinkage due to calcination. The pore diameter is approximately 800 nm. The material is crystalline as revealed by the X-ray diffraction (XRD) pattern (Figure 5.3). TiO_2 in this porous structure is in the anatase phase with a=14.3858; c=4.8429 Å. Macroporous TiO_2 obtained by the $TiCl_4$ route gave an ordered structure as well, as can be seen from the SEM image in Figure 5.2(b), but the material was X-ray amorphous. There was little shrinkage of the pores in this case. By carrying out the hydrolysis around 65°C, one obtains the rutile phase.[92] A SEM image of ordered macroporous zirconia is shown in Figure 5.1(b). The material is crystalline as evidenced by the XRD pattern (Figure 5.3). ZrO_2 has the expanded monoclinic structure (a=6.0522; b=7.6176; c=3.388 Å, β=111.539°). The image in Figure 5.1(b) shows small circular windows approximately

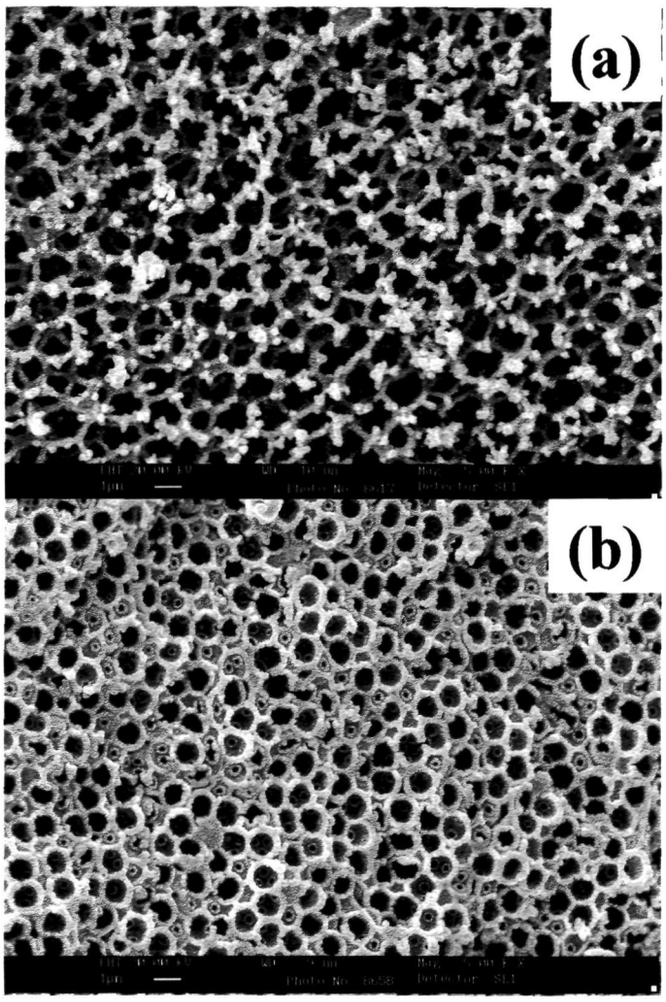

Figure 5.1. (a) SEM image of ordered macroporous SiO_2. (b) SEM image of ordered macroporous ZrO_2.

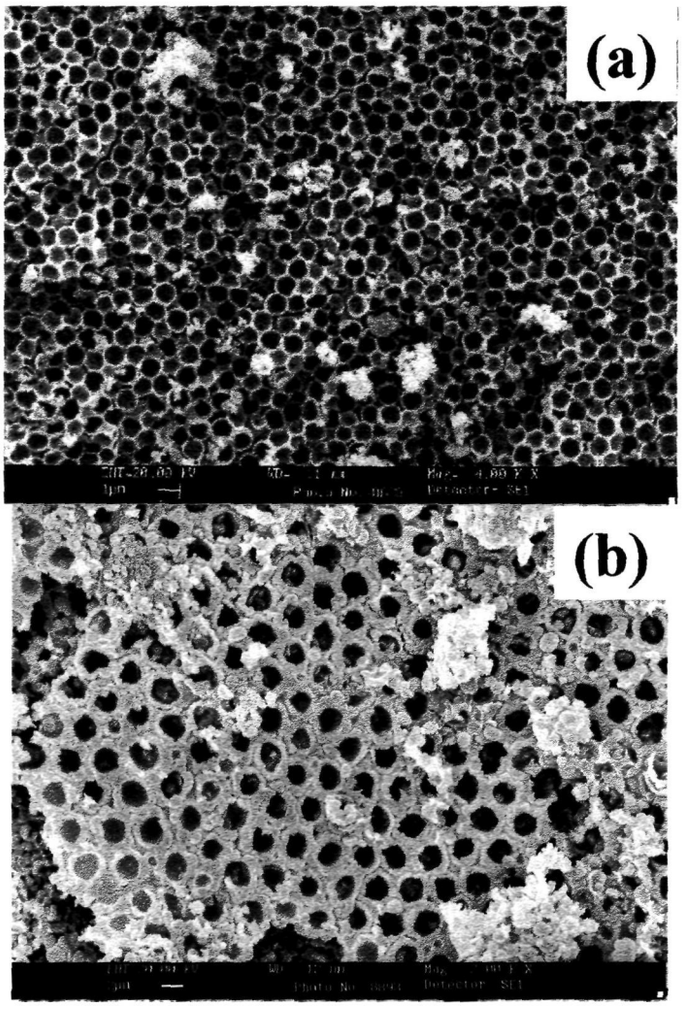

Figure 5.2. SEM images of ordered macroporous TiO_2 obtained by two different routes.

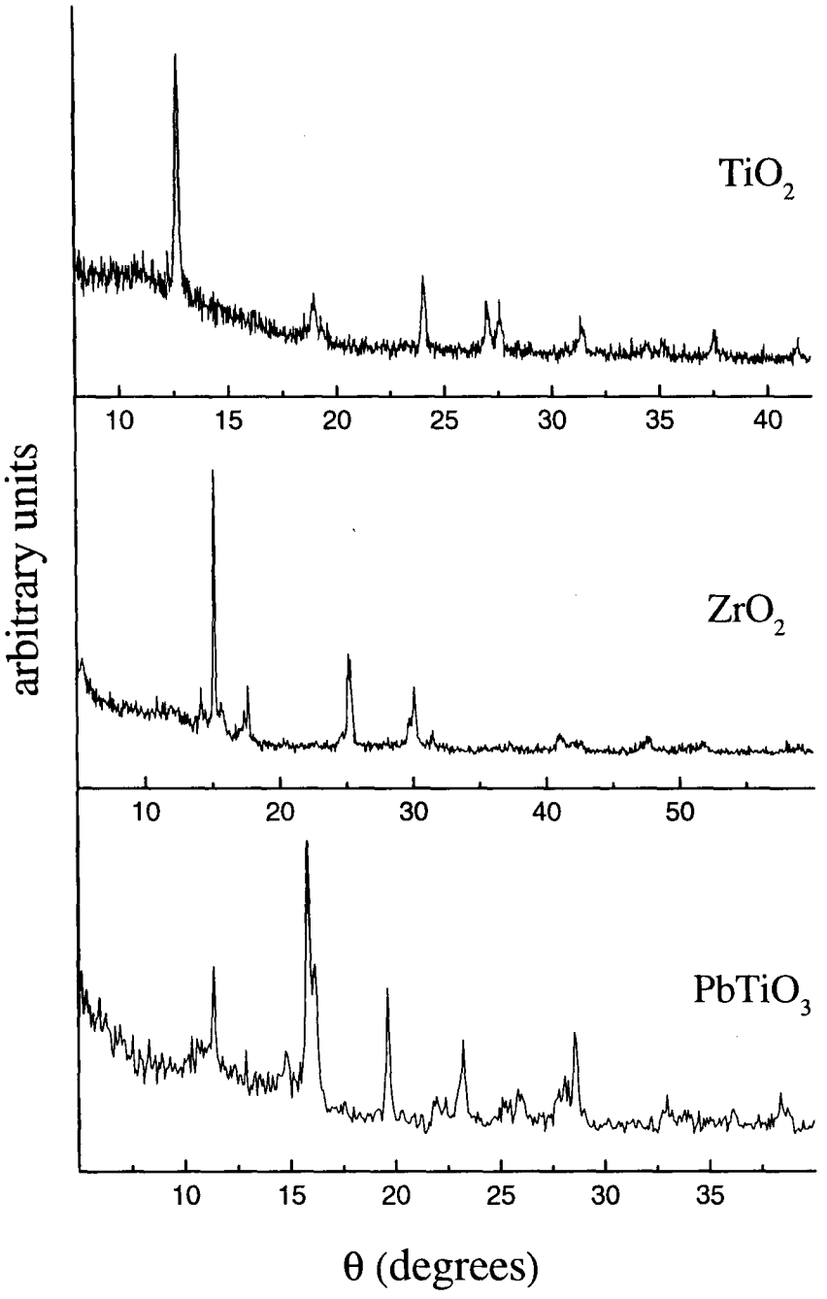

Figure 5.3. XRD patterns of macroporous SiO_2, TiO_2, $PbTiO_3$.

one-quarter the diameter of the big pores. The windows connect the spherical voids and are formed when the close packed spheres are in contact.

The as-prepared macroporous network of $PbTiO_3$ was amorphous. However, on heating at 400°C for 2 hours it became crystalline as evidenced by the XRD pattern shown in Figure 5.3 (tetragonal: a=7.8151; c=4.0984 Å). The stoichiometry was verified by EDX analysis. There was no shrinkage of the pores in the network and we show the porous structure in Figure 5.4(a).

The SEM image of the macroporous structure of $Pb(ZrTi)O_3$ obtained by us is shown in Figure 5.4(b). The material was however X-ray amorphous. Heating the material for purpose of crystallization destroyed the porous structure.

In summary, we have prepared three-dimensional ordered macroporous structures, with pore diameters of 1000 nm, of not only binary oxides, but also of ternary oxides such as ferroelectric $PbTiO_3$. Since gels give good macroporous solids, the scope of this technique is immense. It appears that washing with a solvent is a better way of removing the template from these structures. The macroporous structures of ferroelectric materials may indeed find useful applications.

5.2 Macroporous carbons.

In Figure 5.5(a) we show the SEM images of the macroporous carbon obtained by templating non-porous silica spheres of ~625 nm diameter. Figure 5.5(b) reveals long-

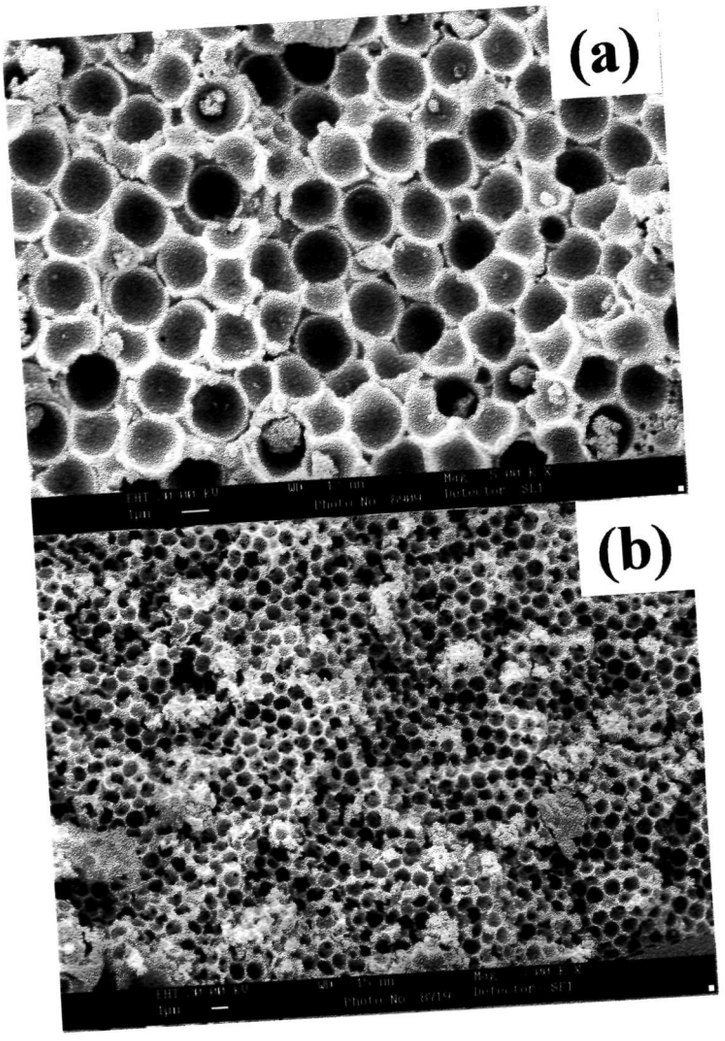

Figure 5.4. (a) SEM image of ordered macroporous $PbTiO_3$.(b) SEM image of ordered macroporous $Pb(ZrTi)O_3$.

range ordering extending to several tens of microns. Thus, the ordering of the templating silica spheres is maintained even after treatment with sucrose, carbonization followed by treatment with aqueous HF. There is considerable shrinkage on removal of the template as seen from Figure 5.5(a) which shows pores of ~400 nm diameter. Similarly, the pores of the carbon sample prepared from silica spheres of ~200 nm diameter, have a diameter of ~125 nm as shown in Figure 5.6. Three-dimensional (3D) ordering is indicated by the circular windows connecting the spheroidal voids, formed when the spheres in the array are in contact with one another. Due to extensive 3D ordering and interconnected voids, these carbon materials are ideal for photonic bandgap applications.

In Figure 5.7(a) we show the reflectance spectra of the silica spheres (~200 nm) coated with carbon as well as the macroporous carbon sample obtained after removal of the silica template. We see a clear maximum at 434 nm for the silica coated with carbon and a maximum at 465 nm for the macroporous carbon sample. These observations are similar to those of Zakhidov and co-workers who observed intense opalescence for their carbon inverse opals prepared by the phenolic and CVD routes.[39] There is a red shift in the wavelength of absorption for the carbon sample due to the increase in the effective refractive index after the silica spheres are removed. Figure 5.7(b) is a photograph of the sample taken under the optical microscope. The colour of the sample was bluish green.

The N_2 adsorption isotherm for the macroporous carbon with ~400 nm diameter pores (prepared by starting with ~625 nm non-porous silica spheres) is shown in Figure

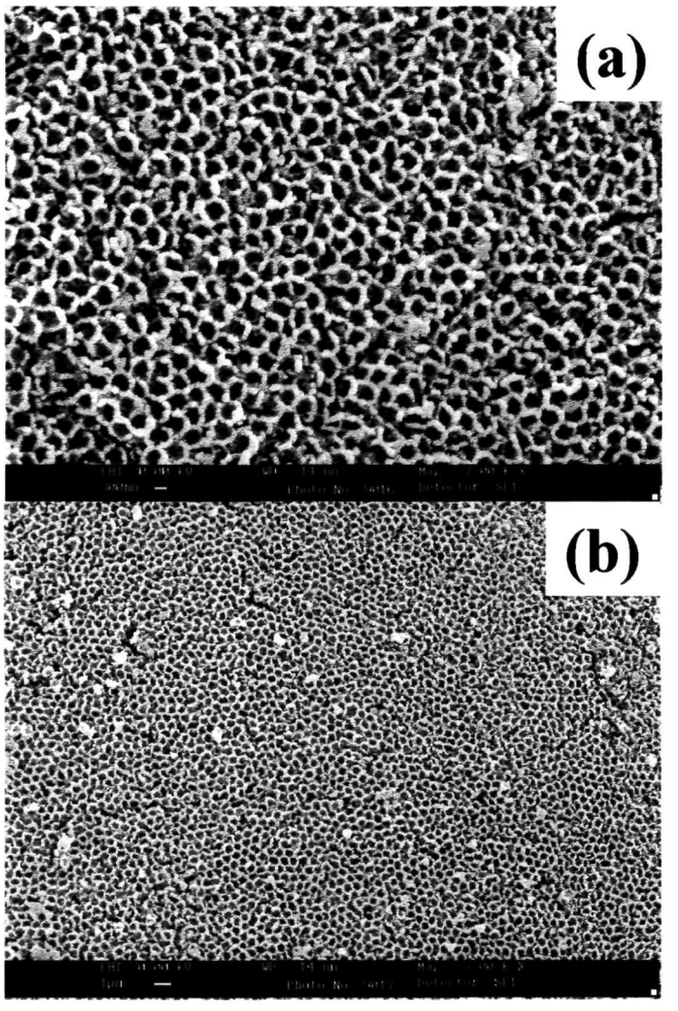

Figure 5.5. (a), (b) SEM images of macroporous carbon obtained by templating non-porous silica spheres of ~625 nm diameter.

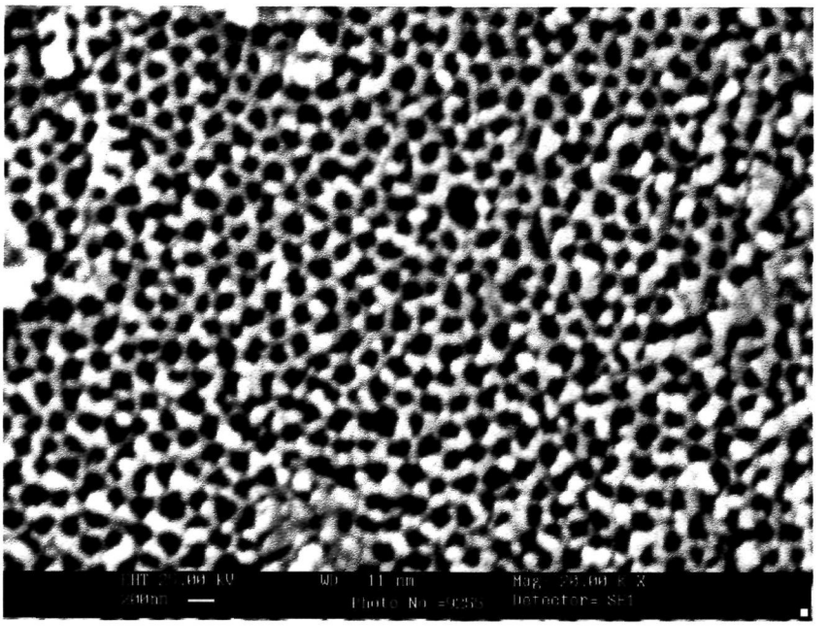

Figure 5.6. SEM image of macroporous carbon obtained by templating non-porous silica spheres of ~200 nm diameter.

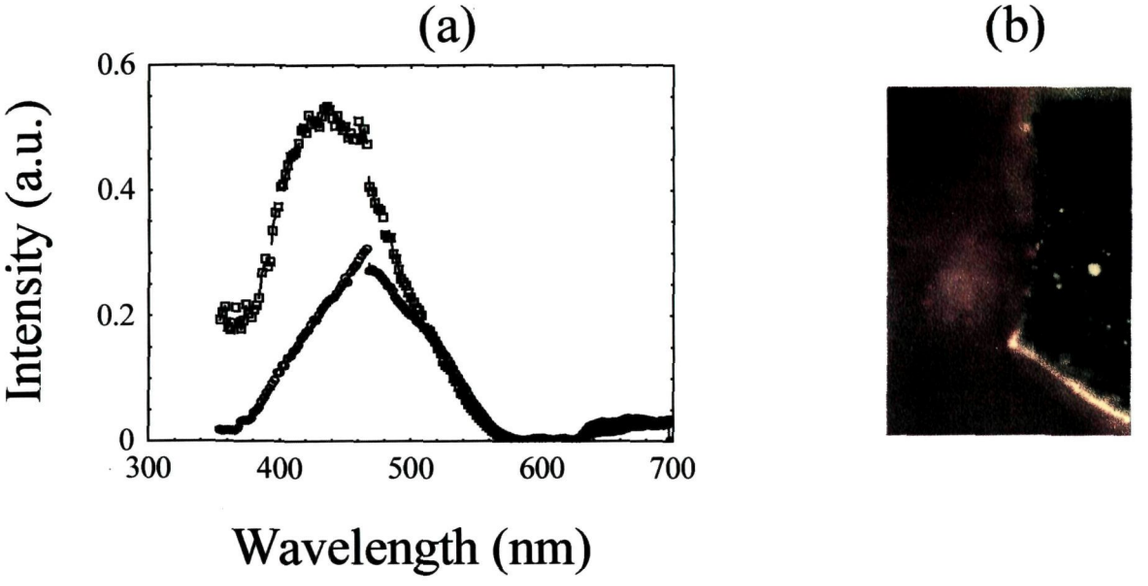

Figure 5.7. (a)Reflectance spectra of silica spheres (~200 nm) coated with carbon and of the carbon network obtained after the removal of the silica spheres (b)Photograph taken in a optical microscope.

5.8(a). It is a typical Type I isotherm, similar to that exhibited by microporous carbons.[93] The slope is high initially, indicating that the micropores get filled at low partial pressures. At higher partial pressures, there is saturation. The surface area calculated by the BET method is 119 m^2g^{-1}. The surface area of the macroporous carbon sample with ~125 nm diameter pores (prepared by starting with ~200 nm non-porous silica spheres) was 226 m^2g^{-1}. Although these values of the surface area are somewhat lower that those of other porous carbons,[93] the presence of ordered macropores may provide certain advantage to macroporous carbons as potential catalyst supports.

The network prepared by templating mesoporous silica spheres (~450 nm diameter) did not show good ordering as the networks obtained with non-porous silica spheres (Figure 5.9(a)). This is mainly because the initial silica arrays themselves are not well ordered. The N_2 adsorption isotherm of the carbon network prepared by templating mesoporous silica spheres was of Type II and gave a surface area of 230 m^2g^{-1}. Since we had started with mesoporous silica spheres, it was expected that the macroporous carbon would have mesoporous walls. However, the mesopores seemed to have been blocked. In order to get a better porous structure, we reduced the sucrose content of the initial reaction mixture to 0.1g. By this means we obtained a macroporous carbon sample exhibiting a N_2 adsorption isotherm of Type I as shown in Figure 5.8(b). The surface area calculated by the BET method was 551 m^2g^{-1}. This value of the surface area is the largest that we have obtained amongst the macroporous carbon samples prepared by us.

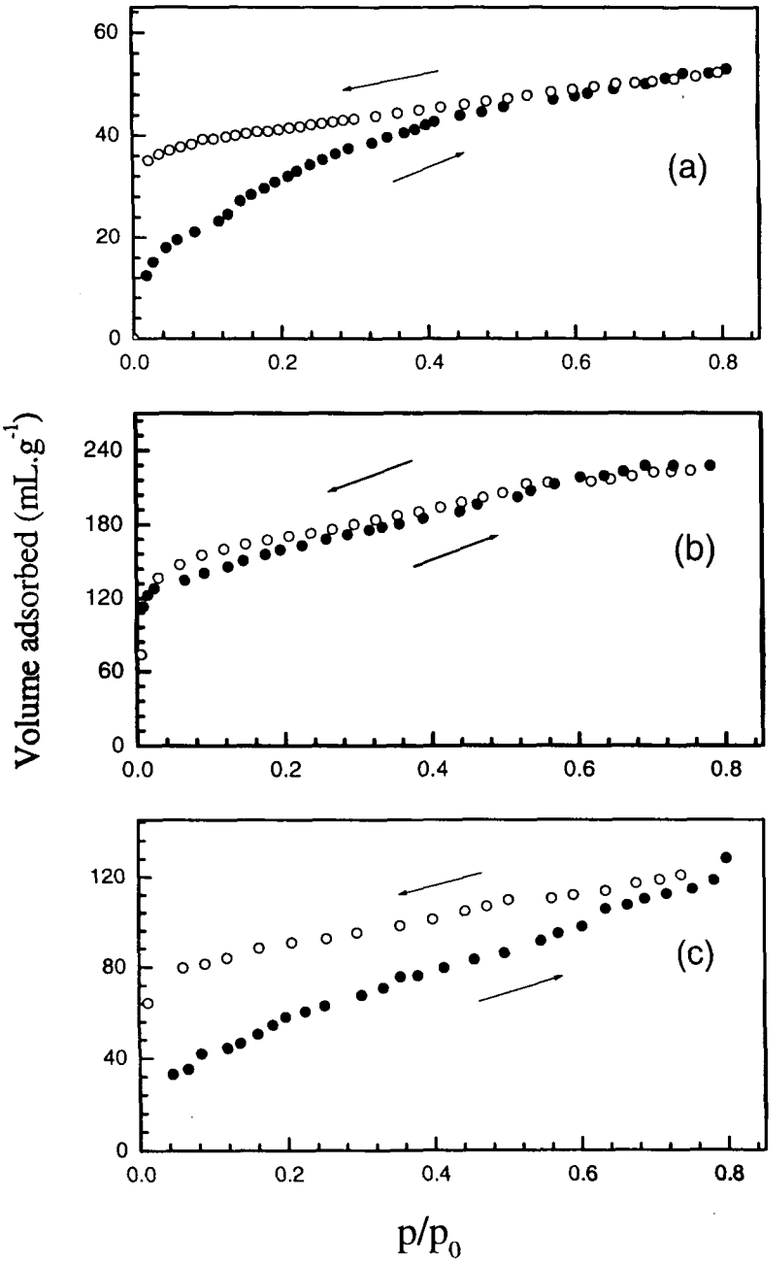

Figure 5.8. N_2 adsorption isotherms for macroporous carbons prepared by templating (a)non-porous silica spheres (~625 nm diameter), (b)mesoporous silica spheres (~450 nm diameter), (c)mixture of 25% mesoporous and 75% non-porous silica spheres.

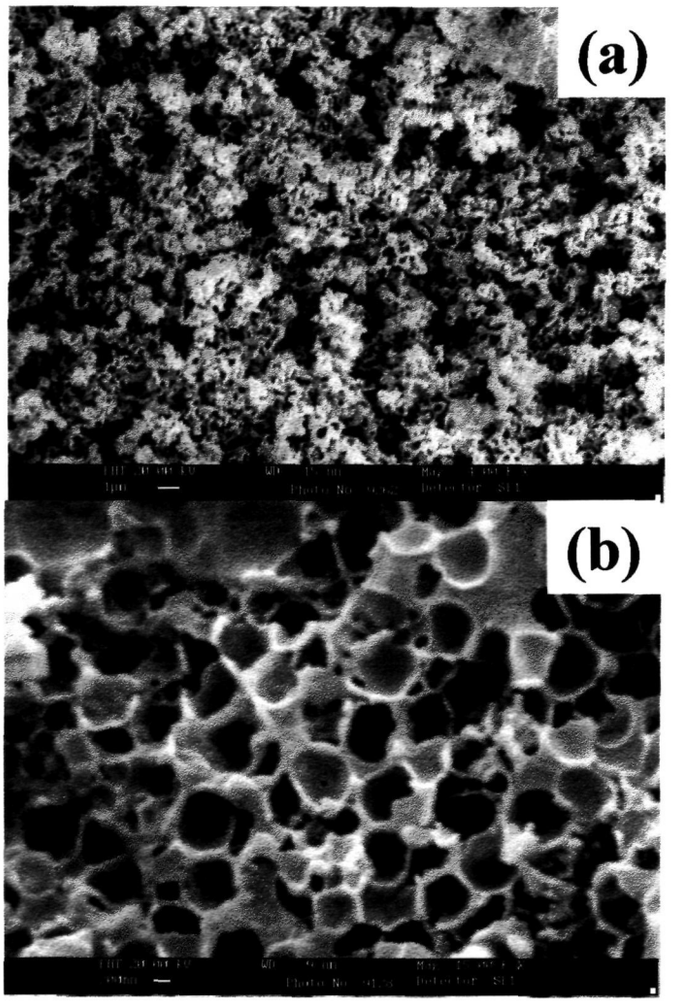

Figure 5.9. SEM image of carbon networks prepared by templating (a)Mesoporous silica spheres and (b)Mixture of mesoporous (25%) and non-porous (75%) silica spheres.

In Figure 5.9(b), we show the SEM image of the macroporous carbon obtained by templating a mixture of 25% mesoporous (~450 nm diameter) and 75% non-porous (~625 nm diameter) silica spheres. Accordingly, we see smaller pores in the SEM image along with the large pores. There is reasonable ordering in this sample, although not as good as in the images shown in Figure 5.5. The N_2 adsorption isotherm of this sample shown in Figure 5.8(c) is of Type II, with a large hysteresis. The BET surface area was 207 m^2g^{-1}, which is in between the values obtained with the samples prepared using non-porous and mesoporous silica spheres.

In summary, we have demonstrated a method for fabricating three-dimensionally ordered macroporous carbon networks. The method can be used to template silica spheres of different sizes with good results, but the surface area of these carbon samples is relatively small. We have templated mesoporous silica spheres by the same method to obtain different porous carbons with somewhat higher surface areas. Although the surface areas of all these macroporous carbons are in the 120-550 m^2g^{-1} range, they could be useful as supports for metal catalysts. The presence of macropores may aid the diffusion of the reacting species to the active sites or of the product to leave the catalyst surface. The 3D ordered macroporous carbons may also be useful as photonic bandgap materials.

5.3 Macroporous silica-alumina composites with mesoporous walls.

Table 5.1 lists the compositions of the various samples prepared by us. In Figure 5.10(a) we show the SEM image of the templating PMMA spheres employed by us. The spheres are of uniform diameter and are ordered into arrays. In Figure 5.10(b) we show the SEM image of sample B after the spheres were treated with the silica-alumina gel, dried and calcined. The networks are fairly well ordered. The diameter of the pores is slightly smaller (~150 nm) than that of the initial PMMA spheres. The shrinkage occurs during the removal of the template during calcination. The SEM image of the samples A and C too were similar to the image in Figure 5.10(b). There was no noticeable change in the external morphology on increasing the amount of aluminum in the samples. The SEM images clearly establish the presence of macropores probably connected in three dimensions.

XRD patterns of the as-synthesized and calcined samples are presented in Figure 5.11. The as-synthesized samples of A, B and C show single peaks with d-values 38.94, 35.26 and 38.15 Å respectively. The low-angle peak is similar to that shown by hexagonal mesoporous solids. There is a decrease in the d-value after calcination due to removal of template CTAB molecules, d-values being 35.5, 32.64 and 33.52 Å respectively for A, B and C. The presence of the low angle peak after calcination indicates that the mesoporous phase is reasonably intact after removal of the template. We know of three materials, A, B, and C, which are macroporous-mesoporous.

	Si/Al		d (Å)		Surface Area (m^2g^{-1})
	gel	**product**	**as-synth.**	**calcined**	
A	18.5	48.0	38.94	35.60	1038
B	12.4	15.3	35.26	32.64	804
C	9.3	4.5	38.15	33.52	676

Table 5.1. Properties of macroporous $SiO_2 - Al_2O_3$ with mesoporous walls

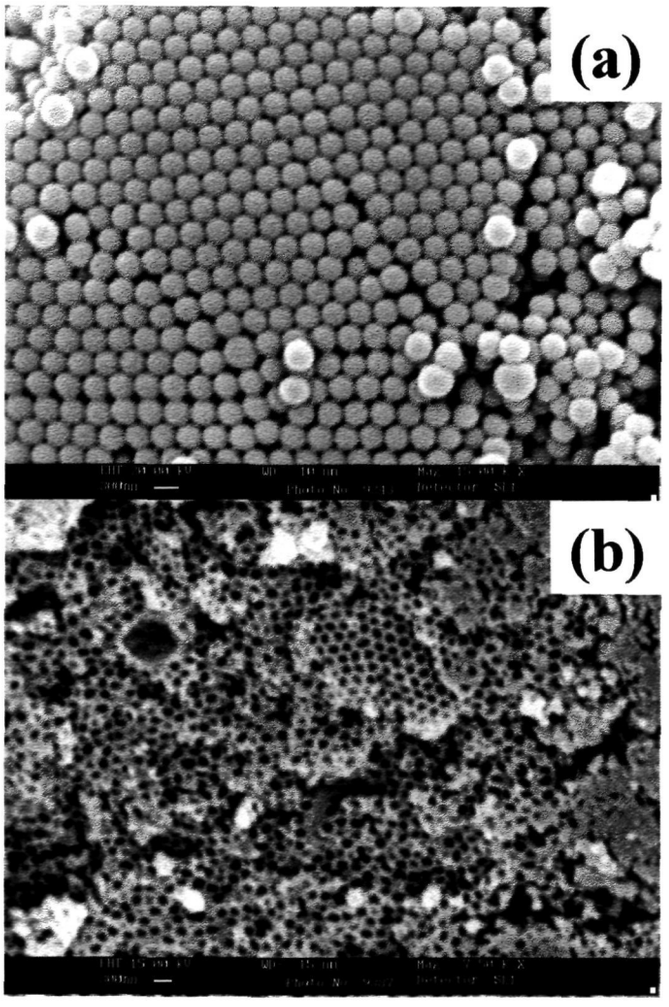

Figure 5.10.(a) SEM image of PMMA spheres of 275nm diameter. (b) SEM image of sample B after removal of the templates

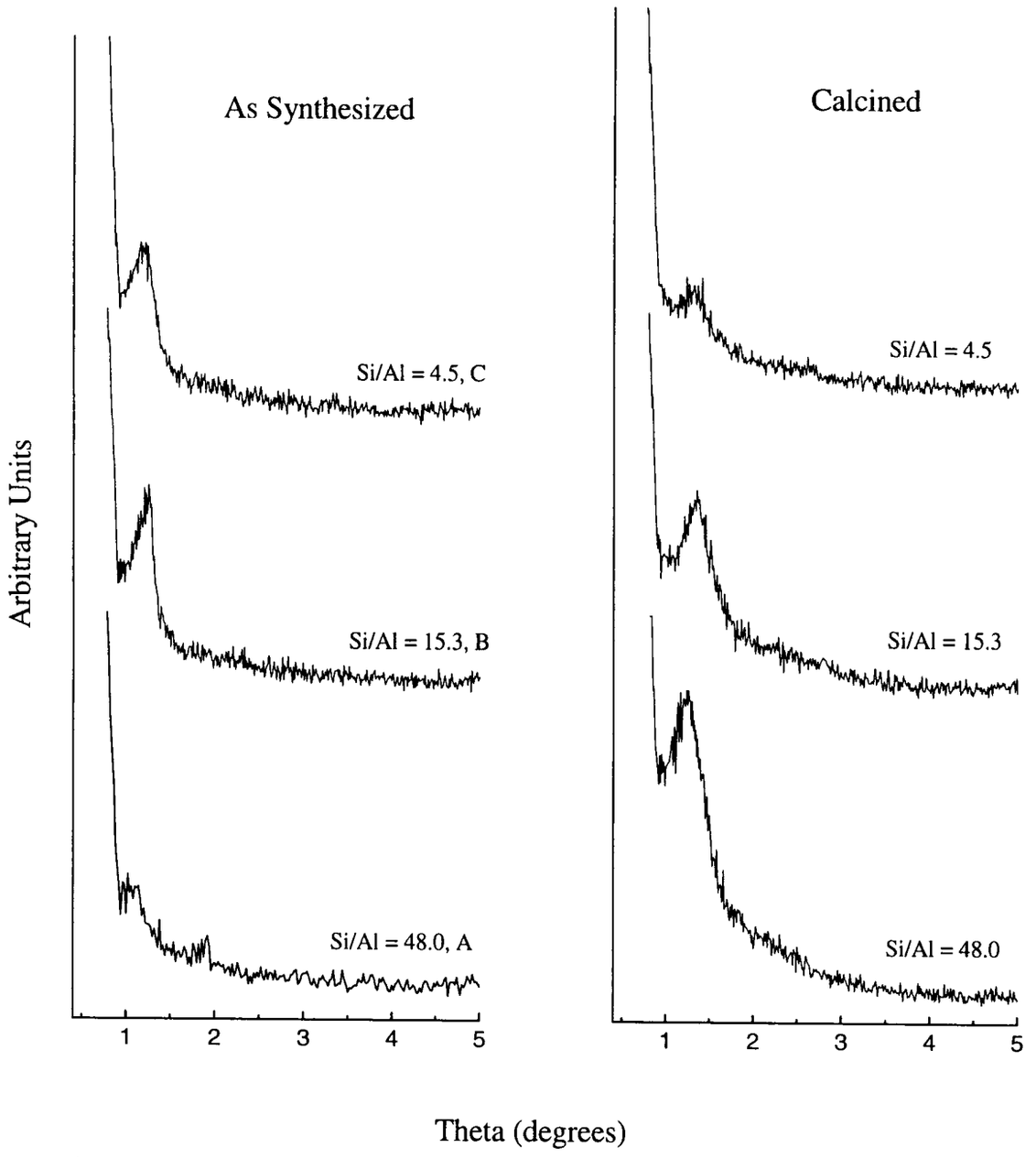

Figure 5.11. XRD patterns of the as-synthesized and calcined samples A, B and C.

TGA curves of the aluminosilicates A and C are shown in Figure 5.12. The as-synthesized samples show a single weight loss from 250-350°C due to the loss of the PMMA and CTAB templates. The weight loss above 350°C is due to the condensation of the silanol that occurs after 350°C. The TGA curve for the calcined samples show a single weight loss corresponding to the adsorbed water. The amount of template removed was calculated to be above 95%.

We performed MAS NMR studies to determine the co-ordination of aluminium and silicon in the framework. ^{29}Si MAS NMR of the as-synthesized sample A showed two broad peaks at –101 and -110ppm corresponding to the Q^3 and Q^4 species respectively. The intensity of the Q^3 species was greater than the Q^4 species indicating that the silanol groups had not condensed fully. On calcination, the relative intensity of the Q^4 species increased, showing that on calcination the silanol groups condense to form Si-O-Si species. ^{27}Al MAS NMR of the calcined sample A showed a large narrow peak at –7ppm corresponding to octahedrally co-ordinated aluminium species and a very small, broad feature centered at 46ppm due to tetrahedrally co-ordinated aluminium. On integrating these peaks, the areas under the peaks were found to be in the ratio of 1:0.2 of the octahedral to the tetrahedral species. It appears only 20% of the Al is present in the framework. Most of the Al is therefore present as Al_2O_3 in composite form with SiO_2. This is because of the limitation due to the pH and temperature employed in the preparation. We may therefore consider A, B, and C as composites of SiO_2 and Al_2O_3 with a small proportion of aluminosilicate. Even though the amount of aluminium in the

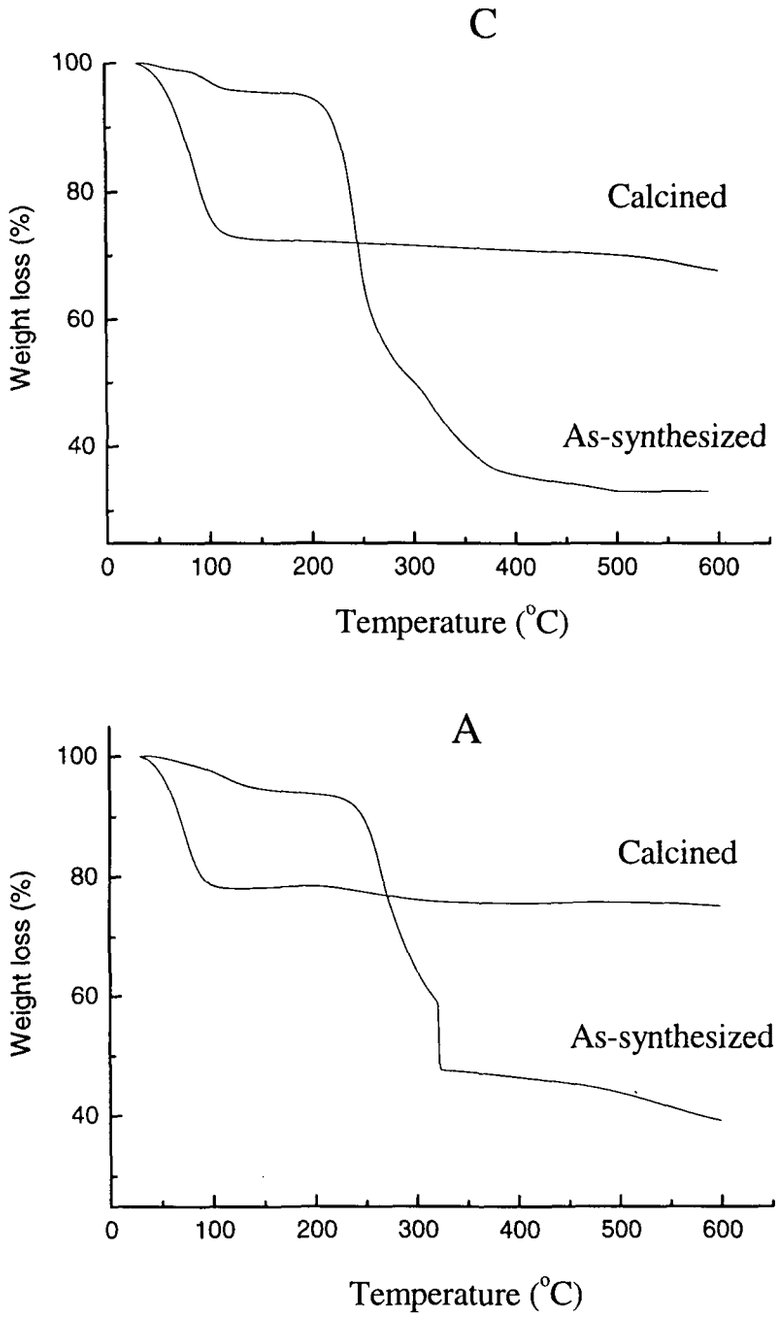

Figure 5.12. TGA curves of the aluminosilicate samples A and C.

framework is small, the composite materials that we have made have macroporous-mesoporous characteristics described earlier.

Nitrogen adsorption isotherms of the samples A,B and C are presented in Figure 5.13. These are typical Type IV isotherms characteristic of mesoporous materials. The isotherms exhibit little or no hysteresis, showing thereby that the pores may not be very ordered. The surface areas calculated by the BET method are in the range of 676-1038 m^2g^{-1} for the three samples. There is a decrease in the surface area with the increasing aluminum content, consistent with the observations of Janicke et. al.,[94] who observed that the surface areas decrease as we decrease the Si/Al ratios.

In summary, we have demonstrated the synthesis of macroporous aluminosilicates containing mesoporous walls. Though the amount of aluminium in the framework is small, the presence of macropores as well as mesopores makes these composites suitable as catalyst supports. The presence of macropores would aid in the diffusion of species to the active sites of the catalyst. The study opens up scope for preparing macroporous-mesoporous structures by doping other transition metals such as Ti, V, Cr, etc. into the silica framework. The only limiting factor is that the reaction has to be carried out at a temperature below which the template decomposes.

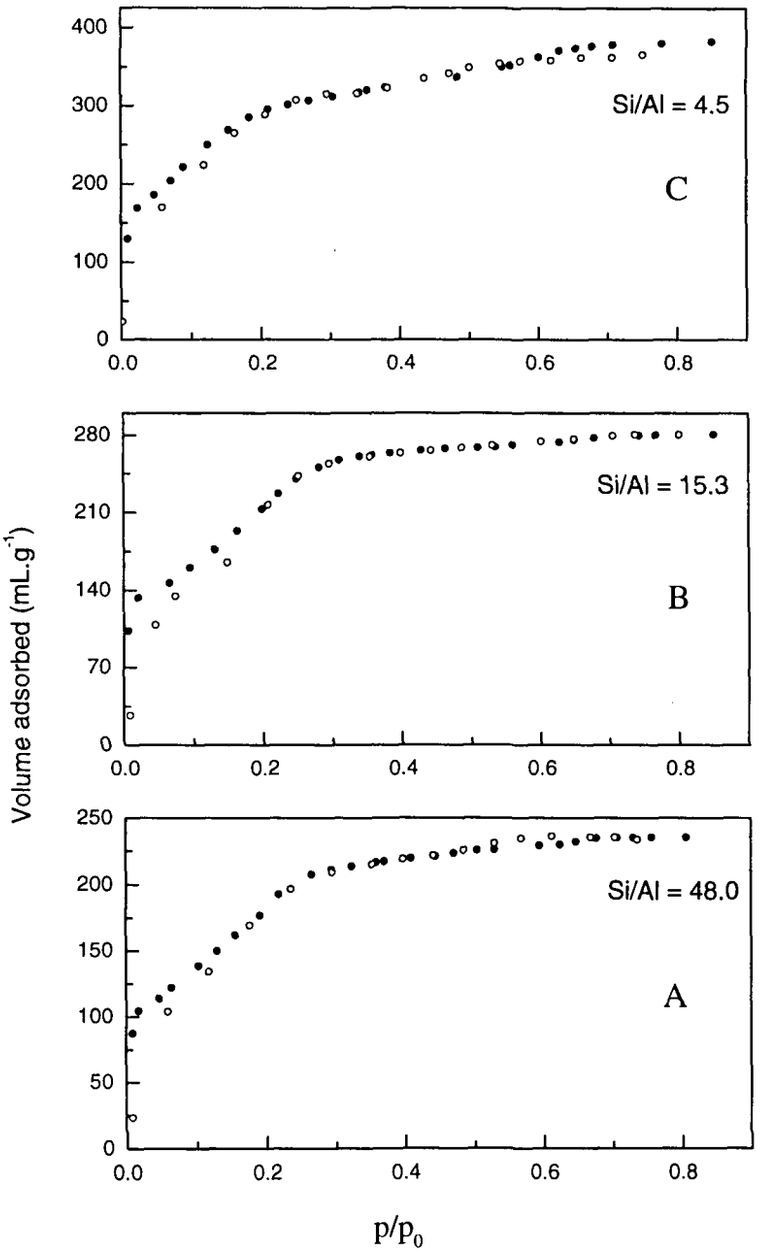

Figure 5.13. N_2 adsorption isotherms for A, B and C. Dark circles represent adsorption cycle and open circles represent desorption cycle.

5.4 Submicron-sized mesoporous aluminosilicate spheres.

Table 5.2 lists the compositions of the various samples prepared by us. Calcination of the spherical aluminosilicates (A-C) and silica (D) at 200°C for 4h removed most of the surfactant template as will be demonstrated later. In Figures 5.14 and 5.15, we show the SEM images of the two aluminosilicate samples with Si/Al ratios of 14 and 40 (A and C respectively). The as-synthesized sample of A with a Si/Al ratio of 14 shows spherical morphology as revealed by the SEM images. There is little agglomeration of particles. The spherical morphology is retained even after calcination at 200°C as can be seen from Figure 5.14(b). This was true of the other two aluminosilicate samples (B and C) as well, as demonstrated in Figure 5.15(b) in the case of sample C. The particles show a narrow size distribution with average diameters 0.35 and 0.30 μm in the case of A and C respectively. The particle sizes of all the samples are listed in Table 5.2.

Powder XRD patterns of the as-synthesized aluminosilicate and silica spheres are presented in Figure 5.16(a). The XRD patterns show a single feature at 2θ values of 2.46°, 2.38°, 2.54° and 2.81° respectively for A, B, C and D. The low-angle peaks are similar to those of hexagonal mesoporous solids. The powder XRD patterns of the samples after calcination at 200°C for 4 hours exhibit single broad peaks at 2θ values of 2.44°, 2.5°, 2.88° and 2.98° respectively for A, B, C and D as revealed in Figure 5.16(b). The shift in the peak positions after calcination is due to the removal of the template. The

Sample	Si / Al[(a)]	d_{100} [(b)] (Å)	Particle diameter (μm)	Surface area (m^2g^{-1})	Pore diameter (Å)
A	14 (49)	35.8 (36.2)	0.35	970	18
B	24 (82)	36.8 (35.3)	0.40	510	15
C	40 (132)	34.8 (30.6)	0.30	700	19
D	Infinity	31.3 (29.6)	0.43	1100	20

(a) The values in parenthesis are obtained after taking into account Al in the framework.

(b) d-value of the low angle reflection in the XRD pattern. The values in brackets were obtained after calcination at 200°C for 4 hours. After calcination at 473 K for 4 hours, the % template removed in the samples is 90-95 %.

Table 5.2. Properties of mesoporous aluminosilicate spheres

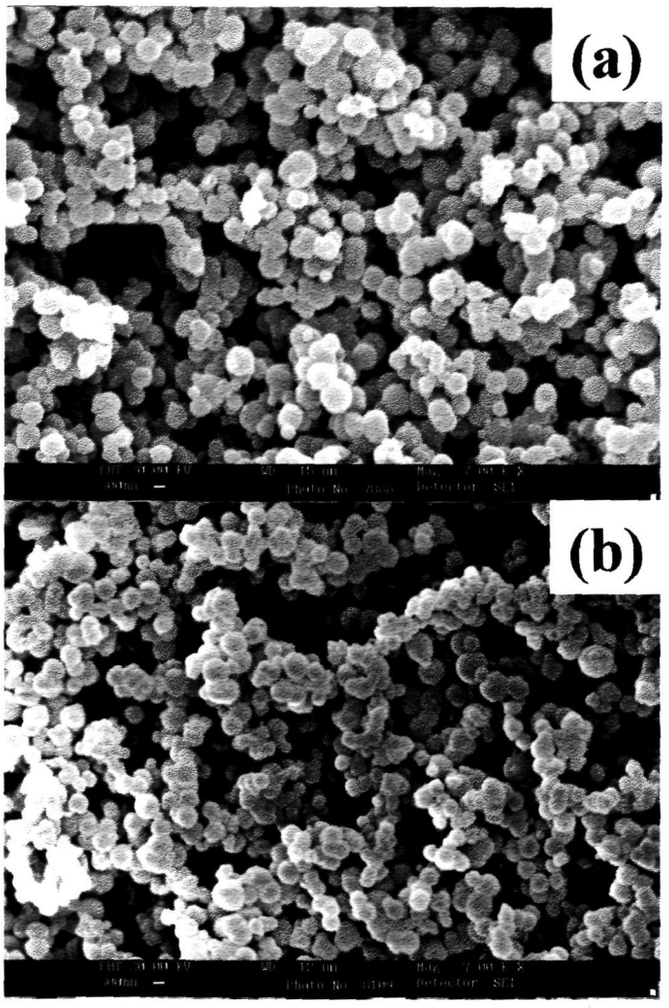

Figure 5.14. SEM micrographs of aluminosilicate spheres A: (a) as-synthesized and (b) after calcination at 200°C for 4h.

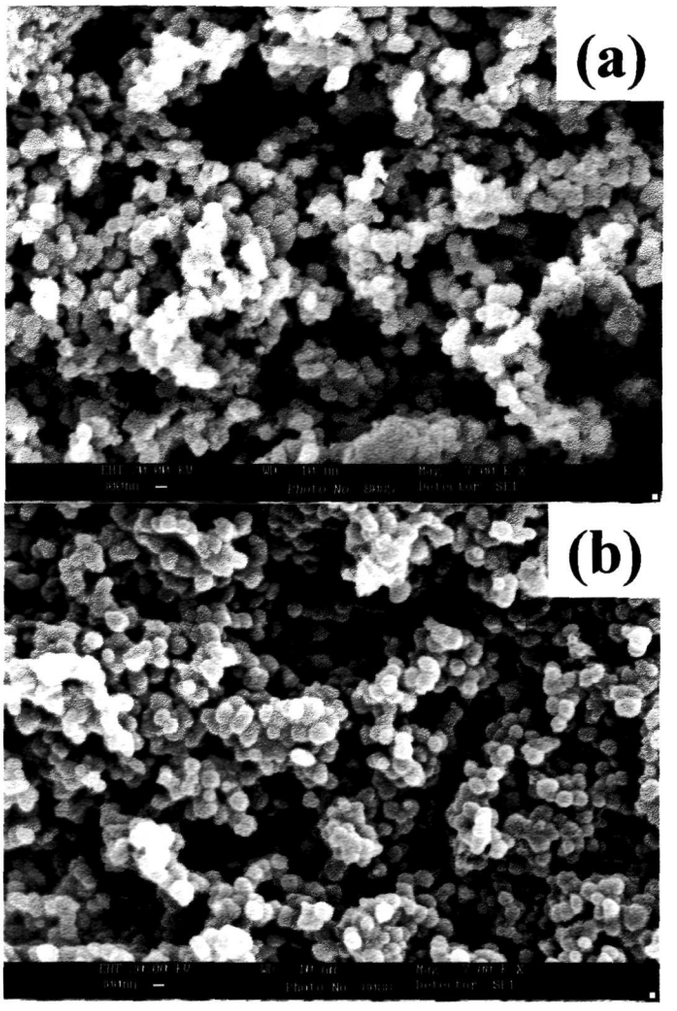

Figure 5.15. SEM micrographs of aluminosilicate spheres C: (a) as-synthesized and (b) after calcination at 200°C for 4h.

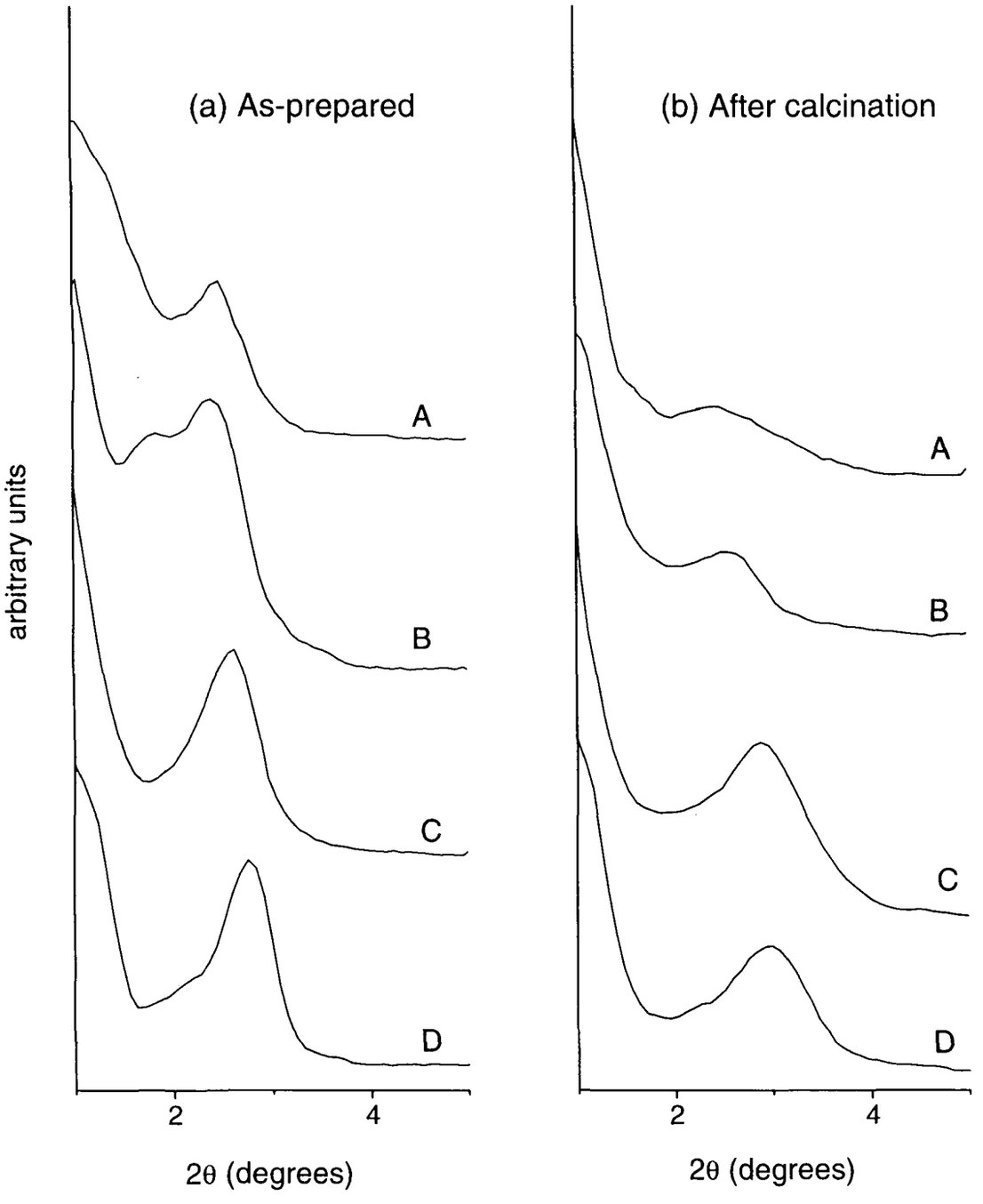

Figure 5.16. XRD patterns for the aluminosilicate (A, B and C) and pure silica (D) spheres

presence of the low-angle reflection after calcination indicates that the mesophase is reasonably intact even after the removal of the template, although the intensity is considerably diminished in the case of the samples A and B. The spherical morphology is, however, retained as mentioned earlier. It appears that the Al-rich samples are more disordered.

TGA curves of the aluminosilicates A and C are shown in Figure 5.17. The as-synthesized samples show one major mass loss in the temperature range 200°-300°C. The mass loss is around 40%, where most of the template is removed. Thus, the sample calcined at 200°C for 4h, only shows a mass loss (<20%) due to adsorbed water around 100°C. The TGA curves confirm that most of the template is removed on calcination at 200°C for 4h. We did not calcine the samples at higher temperatures in order to ensure that the morphology and surface area of the samples are not badly affected. The values of the percentage template removed on calcination 200°C are listed in Table 5.2. The values are in the range 87-95%.

^{29}Si and ^{27}Al MAS NMR spectra of sample C are shown in Figure 5.18. The ^{29}Si NMR spectrum of the as-synthesized sample shows two peaks at –100 and –108 ppm due to the Q^3 and Q^4 silicate species respectively. The intensity of the Q^3 species is greater than that of the Q^4 species indicating that the silanol groups have not condensed fully. On calcination, however, the relative intensity of the Q^4 species increases, showing that the silanol groups condense to form the Si-O-Si species. The ^{27}Al NMR spectrum of the as-synthesized samples show two peaks at 47 and 9.5 ppm. These are due to tetrahedrally

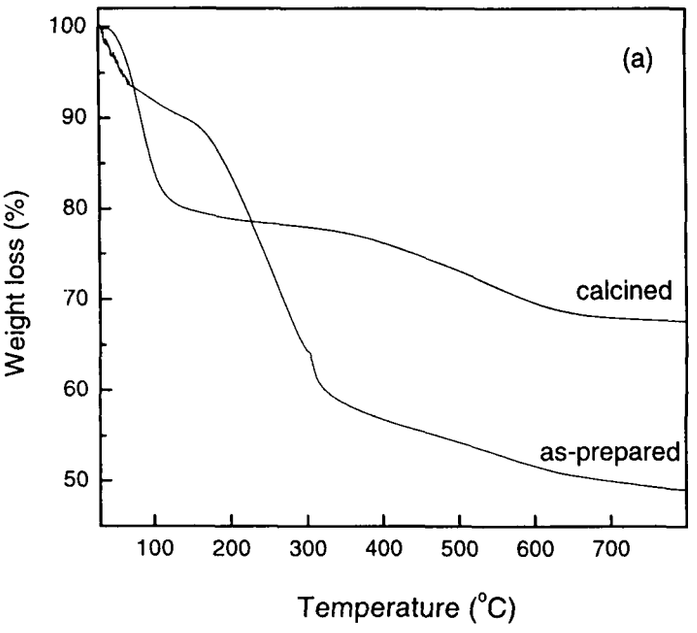

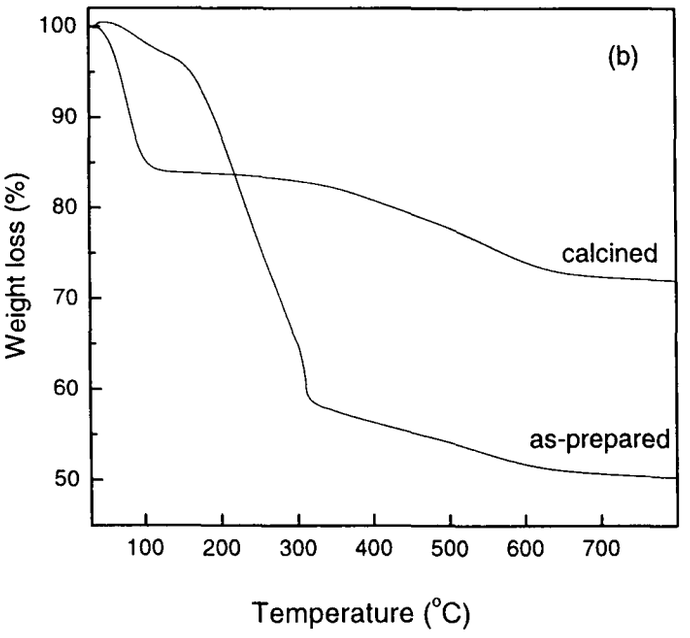

Figure 5.17. TGA curves of the aluminosilicate samples A and C.

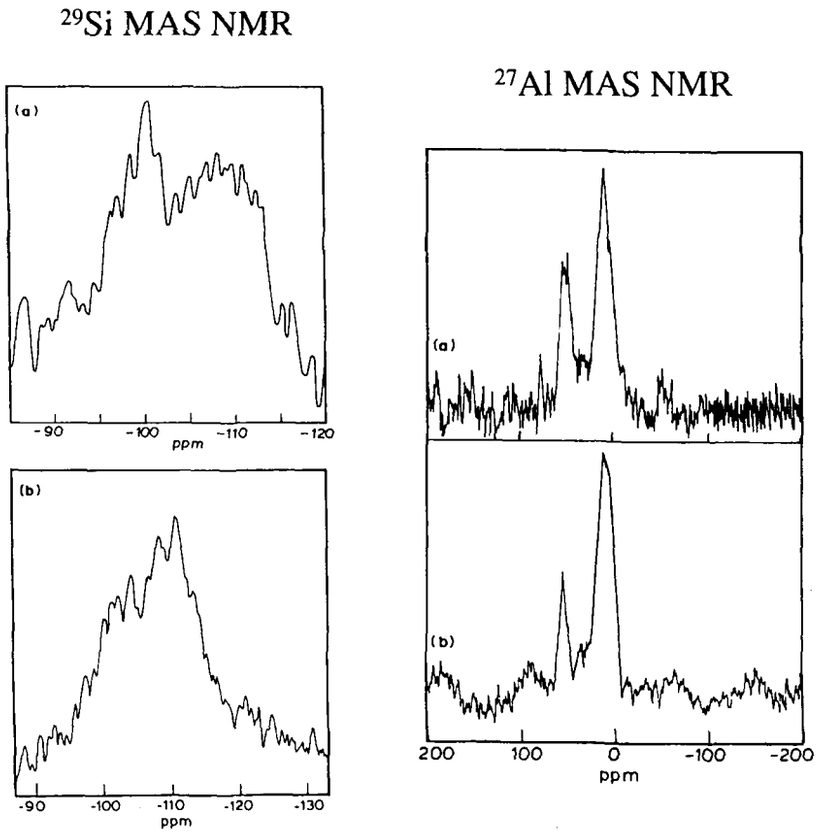

Figure 5.18. MAS NMR spectra of sample C
(a)as-synthesized and (b)after calcination.

octahedrally co-ordinated species respectively. After calcination, the relative proportion of the peaks corresponding to the tetrahedral and the octahedral species remains the same. Taking account of only the tetrahedral species to be a part of the framework, we estimate the percentage of aluminium in the framework to be around 30%. The Si/Al ratios calculated on this basis are listed in Table 5.2.

Nitrogen adsorption isotherms of samples A and C are presented in Figure 5.19. These are typical type IV adsorption isotherms. The BET surface areas of the samples calculated from N_2 adsorption are in the range 500-1000 m^2g^{-1} (Table 5.2). In general, the surface area of the aluminosilicate spheres is smaller than that the pure silica spheres. The pore size distribution was calculated using the BJH method. In Figure 5.20, we show the plots of the pore size in case of samples A and C. The particles have a narrow pore size distribution, the values of the pore diameters being in the range 15-20 Å (Table 5.2). The pore size of the aluminosilicate spheres is smaller than that of the pure silica spheres. We could estimate the diameter of the pores from the low-angle XRD peaks by making use of the relation $a_o=(2d_{100})/(3)^{1/2}$.The values of the diameter obtained are considerably larger than the pore diameter from adsorption measurements, since the former includes the wall thickness. We have estimated the wall thickness from the difference in the XRD (a_o) and adsorption pore diameters. These values are in the 7-13 Å range, the thickness increasing with Al content.

In summary, the present work demonstrates that it is possible to prepare submicron-sized mesoporous spheres of aluminosilicates by using surfactant templating.

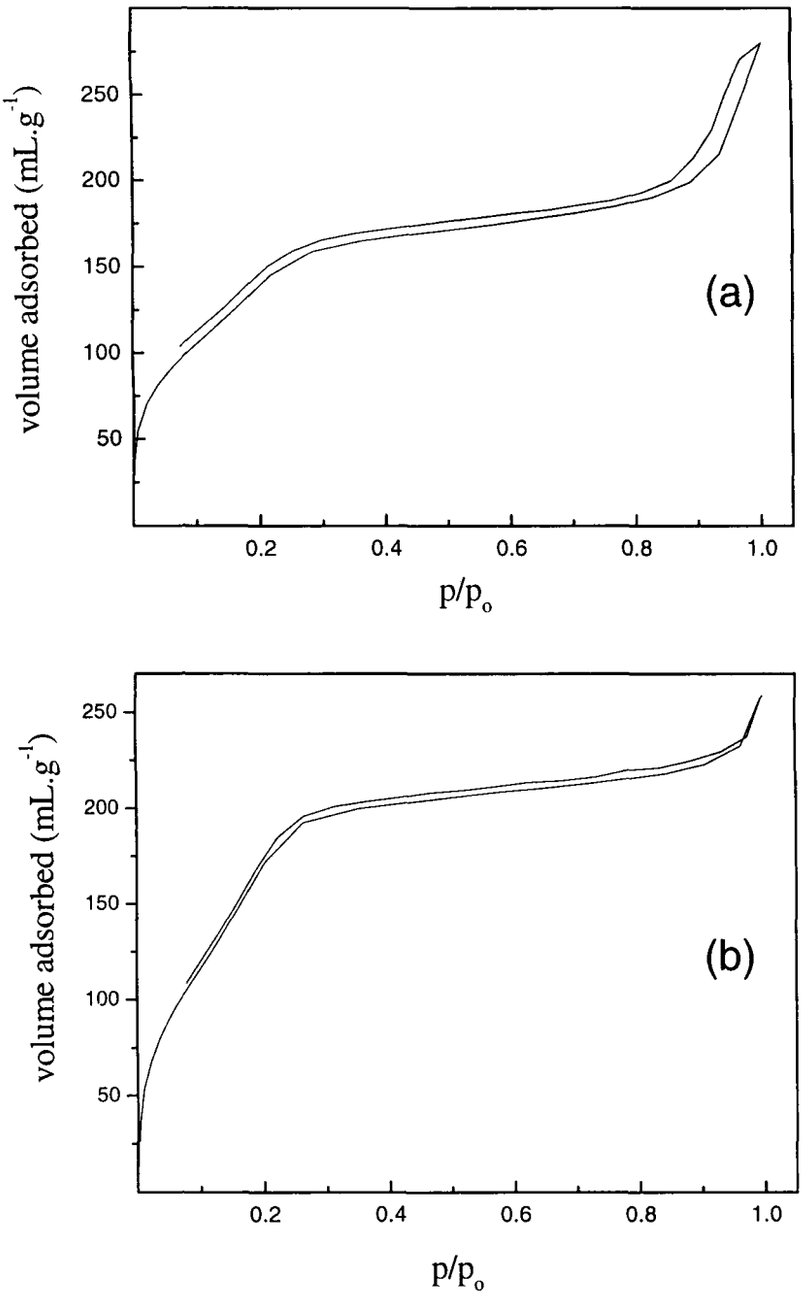

Figure 5.19. N_2 adsorption isotherms for samples (a)A and (b)C.

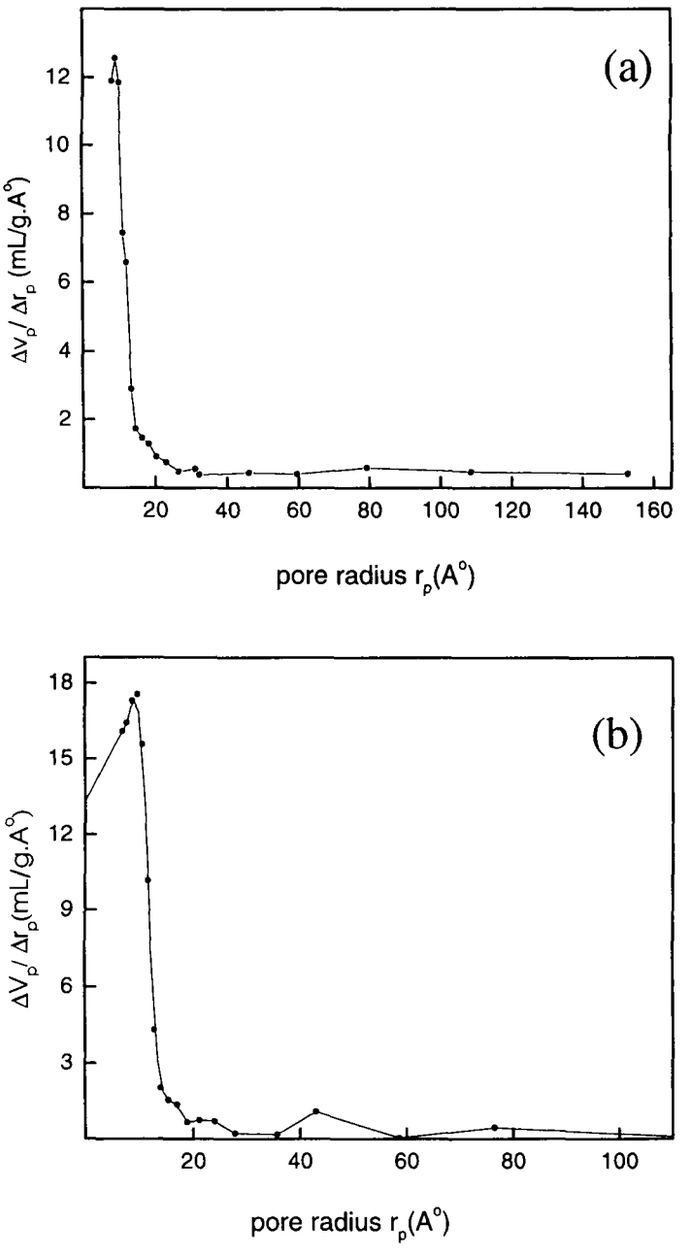

Figure 5.20. Pore size distribution for the samples a)A and (b)C.

Although the sample crystallinity is not as high as in the case of pure silica spheres prepared by a similar procedure, the high surface areas and desirable pore diameters of the aluminosilicate spheres make them good candidates for use in catalysis, sorption and related applications.

REFERENCES

1. R. R. Bhave, *Inorganic Membranes: Synthesis, Characteristics and Applications,* Van Nostrand Reinhold, New York, **1991**.
2. D. E. Fain, *MRS Bull.*, **1994**, *19*, 40.
3. Y. Lin, S-Y. K. Motesharie, K. P. S. Dancil, M. J. Sailor and Ghadiri, *Science,* **1997**, *278,* 840.
4. J. D. Joannopoulos, P. R. Villeneuve and S. Fan, *Nature,* **1997,** *386,* 143.
5. D. W. Schaefer, *MRS Bull.*, **1994**, *19*, 14.
6. M. E. Davis and R. F. Lobo, *Chem. Mater.*, **1992**, *4,* 756.
7. (a) J. M. Thomas, *Angew. Chem. Int. Ed. Engl.*, **1999**, *38*, 3588 ; (b) A. K. Cheetham, G. Ferey and T. Louseau, *Angew. Chem. Int. Ed. Engl.*, **1999**, *38*, 3588.
8. C. T. Kresge, M. E. Leonowicz, W. J. Roth, J. C. Vartuli and J. S. Beck, *Nature*, **1992**, *359*, 710.
9. J. S. Beck, J. C. Vartuli, W. J. Roth, M. E. Leonowicz, C. T. Kresge, K. D. Schmidt, C. T.-W. Chu, D. H. Olson, E. W. Sheppard, S. B. Mccullen, J. B. Higgins and J. L. Schlenker, *J. Am. Chem. Soc.,* **1992**, *114,* 10834.
10. P. Behrens, *Angew Chem Int. Ed. Engl.*, **1996**, *35*, 515 and references therein.
11. S. A. Bagshaw and T. J. Pinnavaia, *Angew. Chem. Int. Ed. Engl.,* **1996**, *35,* 1102.
12. D. M. Antionelli and Y. J. Ying, *Angew. Chem. Int. Ed..,* **1995**, *34,* 2014.
13. S. Ayyappan, N. Ulagappan and C. N. R. Rao, *J. Mater. Chem.,* **1996**, *6*, 1737.
14. N. Ulagappan and C. N. R. Rao, *Chem. Commun.,* **1996**, 1685.
15. S. Neeraj and C. N. R. Rao, *J. Mater. Chem.* , **1998**, *8*, 1631.
16. S. Neeraj, M. Eswaramoorthy and C. N. R. Rao, *Mat. Res. Bull*, **1998**, *38*, 1549.
17. B. Chakraborty, A. C. Pullikottil, S. Das and B. Viswanathan, *Chem. Commun.,* **1997**, 911.
18. P. Feng, Y. Xia, J. Feng, X. Bu and G. D. Stucky, *Chem. Commun.,* **1997**, 949.
19. S. Schacht, Q. Hou, I. G. Voigtmartin, G. D. Stucky and F. Schüth, *Science,* **1996**, *273*, 768.
20. H. Yang, N. Coombs, I. Sokolov and G. A. Ozin, *Nature*, **1996**, *381*, 589.
21. H. Yang, V. Gregory, N. Coombs, S. Igor and G. A. Ozin, *J. Mater. Chem.* **1998**, *8,* 743.

22. K. Schumacher, M. Grün and K. K. Unger, *Micro. and Meso. Mat.*, **1999**, *27*, 201.
23. C. Y. Chen, S. L. Burkett, H. X. Li and M. E. Davis, *Microporous Mat.*, **1993**, *2*, 27.
24. Q. Huo, D. I. Margolese, U. Ciesla, D. G. Demuth, P. Feng, T. E. Gier, P. Sieger, A. Firouzi, B. F. Chmelka, F. Schüth and G. D. Stucky, *Chem Mater.*, **1994**, *6, 1176.*
25. N. Ulagappan and C. N. R. Rao, *Chem. Commun.*, **1996**, 2759.
26. A. Corma, Q. Kan, M. Navarro, J. Perez-Pariente and F. Rey, *Chem. Mater.*, **1997**, 2123.
27. D. Khushalani, A. Kuperman, G. A. Ozin, K. Tanake, J. Graces, M. M. Olken and N. Coombs, *Adv. Mater.*, **1995**, *7*, 842.
28. B. T. Holland, C. F. Blanford and A. Stein, *Science*, **1998**, *28*, 538.
29. P. T. Tanev, M. Chibwa and T. Pinnavaia, *Nature*, **1994**, *368*, 321.
30. H. W. Ballew, *Am. Biotechnol. Lab.*, **1997**, *May,* 8.
31. J. A. Hubbell and R. Langer, *Chem. Eng. News,* **1995**, *March 13, 42.*
32. R. C. Furneaux, W. R. Rigby and A. P. Davidson, *Nature*, **1989**, *337*, 147.
33. R. J. Tonucci, B. L. Justus, A. J. Campillo and C. E. Ford, *Science*, **1992**, *258*, 783.
34. M. Yoshida, M. Asano, T. Suwa, N. Reber, R. Spohr and R. Katakai, *Adv. Mater.*, **1997**, *9*, 757.
35. G. Widawski, M. Rawiso and B. Francois, *Nature,* **1994**, *369*, 387.
36. D. J. LeMay, R. W. Hopper, L. W. Hrubesh and R. W. Pekara, *MRS Bull.*, **1990**, *15*, 19.
37. B. Gates, Y. Yin and Y. Xia, *Chem. Mater.*, **1999**, *11*, 2827.
38. P. Jiang, K. S. Hwang, D. M. Mittleman, J. F. Bertone, and V. L. Colvin, *J. Am. Chem. Soc.*, **1999**, *121,* 11629.
39. A. A. Zakhidov, R. H. Baughman, Z. Iqbal, C. Cui, I, Khyarullin, S. O. Dantas, J. Marti and V. G. Rakihenko, *Science*, **1998**,*282,* 897.
40. J. E. G. J. Wijnhoven and William L. Vos, *Science*, **1998**, *281*, 802.
41. O. D. Velev, T. A. Jede, R. F. Lobo and A. M. Lenhoff, *Nature*, **1997**, *389*, 447.
42. B. T. Holland, C. F. Blanford, T. Do and A. Stein, *Chem. Mater.*, **1999**, *11*, 795.
43. A. Imhof and D. J. Pine, *Nature*, **1999**, *389*, 948.
44. H. Yan, C. F. Blanford, W. H. Smyrl and A. Stein, *Chem. Commun.*, **2000**, 1477.
45. E. Matijevic, *Acc. Chem. Res.*, **1981**, *14*, 22.

46. W. Stöber and A. Fink, *J. Colloid. Interface Sci.*, **1968**, *26*, 62.

47. R. K. Iler, *the Chemistry of Silica*, Wiley, New York, **1979**.

48. D. W. McComb, B. M. Treble, C. J. Smith, R. M. De La Rue and N. P. Johnson, *J. Mater. Chem.*, **2001**, *11*, 142.

49. *Emulsion Polymerization* (Ed: I. Piirma), Academic, New York, **1982.**

50. D. H. Everett, *Basic Principles of Colloid Science*, Royal Society of Chemistry, London, **1988**.

51. J. V. Sanders, *Nature*, **1964**, *204*, 1151.

52. H. Miguez, F. Meseguer, C. Lopez, A. Mifsud, J. S. Moya and L. Vazquez, *Langmuir*, **1997**, *13*, 6009.

53. L. V. Woodcock, *Nature,* **1997**, *388*, 235.

54. D. H. Van Winkle and C. A. Murray, *Phy. Rev.*, **1986**, *34*, 562.

55. S. Park and Y. Xia, *Langmuir*, **1999**, *15*, 266.

56. A. Blanco, E. Chomski, S. Grabtchak, M. Ibisate, S. John, S. W. Leonard, C. Lopez, F. Meseguer, H. Miguez, J. P. Mondia, G. A. Ozin, O. Toader and H. M. van Driel, *Nature,* **2000**, *405*, 437.

57. P. Jiang, J, Cizeron, J. F. Bertone and V. L. Colvin, *J. Am. Chem. Soc.*, **1999**, *401,* 548.

58. O. D. Velev, P. M. Tassier, A. M. Lenhoff and E. W. Kaler, *Nature*, **1999**, *401*, 548.

59. P. Jiang, K. S. Hwang, D. M. Mittleman, J. F. Bertone and V. L. Colvin, *J. Am. Chem. Soc.*, **1999**, *121*, 11633.

60. M. Antonietti, B. Berton, C. Göltner and Hans-Peter Hentze, *Adv. Mater.*, **1998**, *10*, 154.

61. B. T. Holland, L. Abrams and A. Stein, *J. Am. Chem. Soc.*, **1999**, *121*, 4309.

62. J. D. Joannopoulos, R. D. Meade and J. N. Winn. *Photonic Crystals,* Princeton University Press, Princeton, NJ, **1995**.

63. S. John, *Phy. Rev. Lett.*, **1987**, *58*, 2486.

64. E. Yablonovitch, *Phy. Rev. Lett.*, **1987**, *58*, 2059.

65. E. Yablonovitch, T. Gmitter and K. Leung, *Phy. Rev. Lett.*, **1991,** *67*, 2295.

66. C. Chan, K. Ho and C. Soukoulis, *Europhy. Lett.*, **1991,** *16*, 563.

67. H. Sözüer and J. Haus, *J. Opt. Soc. Am. B*, **1993**, *10,* 296.

68. K. Ho, C. Chan, C. Soukoulis, R. Biswas and M. Sigalas, *Solid State Commun.*, **1994**, *89*, 413.

69. H. Sözüer and J. Dowling, *J. Mod. Opt.*, **1994**, *41*, 231.

70. A. D. Dinsmore, J. C. Crocker and A. G. Yodh, *Curr. Opin. Colloid Interface. Sci.*, **1998**, *3*, 5.

71. M. S. Thijssen, R. Sprik, J. E. G. J. Wijnhoven, M. Megens, T. Narayanan, A. Lagendijk and W. L. Vos, *Phy. Rev. Lett.*, **1999**, *83*, 2730.

72. K. Yashino, S. B. Lee, S. Tatsuhara, Y. Kawagishi, M. Ozaki and A. A. Zakhidov, *Appl. Phy. Lett.*, **1998**, *74*,. 3506.

73. G. Subramania, K. Constant, R. Biswas, M. M. Sigalas and K.-M. Ho., *Appl. Phy. Lett.*, **1999**, *74*, 3933.

74. E. Yablonovitch, *J. Opt. Soc. Am. B*, **1993**, *10*, 283.

75. K. Busch and S. John, *Phy. Rve. E*, **1998**, *58*, 3896.

76. L. V. Woodcock, *Nature*, **1997**, *385*, 141.

77. P. N. Pusey, W. van Megen, P. Bartlett, B. J. Ackerson, J. G. Rarity and S. M. Underwood, *Phy. Rev. Lett.*, **1989**, *63*, 2753.

78. H. Miguez, F. Meseguer, C. Lopez, A. Mifsud, J. S. Moya and L. Vazquez, *Langmuir*, **1997**, *13*, 6009.

79. D. W. McComb, B. M. Treble, C. J. Smith, R. M. De La Rue and N. P. Johnson, *J. Mater. Chem.*, **2001**, *11*, 142

80. J. F. Bertone, P. Jiang, K. S. Hwang, D. M. Mittleman and V. L. Colvin, *Phy. Rev. Lett.*, **1999**, *83*, 300.

81. B. Gates, S. H. Park and Y. Xia, *J. Lightwave Technol.*, **1999**, *17*, 1956.

82. Y. A. Vlasov, N. Yao and D. J. Norris, *Adv. Mater.*, **1999**, *11*, 165.

83. P. V. Braun and P. Wiltzius, *Nature*, **1999**, *402*, 603.

84. G. Subramanian, V. N. Manoharan, J. D. Thorne and D. J. Pine, *Adv. Mater.*, **1999**, *11*, 1261.

85. R. Ryoo, S. H. Joo and S. Jun, *J. Phy. Chem. B*, **1999**, *103*, 7743.

86. K.K Unger, H. Giesche and J.N. Kinkel, *German Patent DE-3534, 143.2*, 1985.

87. C. Kaiser and K. K. Unger, *German Patent DE-195 30031 A1*, 1997.

88. G. Büchel, K. K. Unger, A. Matsumoto and K. Tsutsumi, *Adv. Mater.*, **1998**, *10*, 1036.

89. Q. Huo, J. Feng, F. Schüth and G. D. Stucky, *Chem. Mater.*, **1997**, *9*, 14.

90. L. Qi, J. Ma, H. Cheng and Z. Zhao, *Chem. Mater.*, **1998**, *10*, 1623.

91. M. Grün, I. Lauer and K. K. Unger, *Adv. Mater.*, **1997**, *9*, 254.

92. S. D. Park, Y.H.Cho, W. W.Kim and S.J.Kim, *J. Solid State Chem.*, **1999,** *146,* 230.

93. J. F. Bryne and H. Marsh, *Porosity in Carbons*, ed. J. W. Partick, Edward Arnold, **1995**, Great Britain.

94. M. T. Janicke, C. C. Landry, S. C. Christiansen, S. Birtalan, G. D. Stucky and B. F. Chmelka, *Chem. Mater.*, **1999,** *11*, 1342.